

UNCLASSIFIED

AD 432182

DEFENSE DOCUMENTATION CENTER

FOR

SCIENTIFIC AND TECHNICAL INFORMATION

CAMERON STATION, ALEXANDRIA, VIRGINIA



UNCLASSIFIED

NOTICE: When government or other drawings, specifications or other data are used for any purpose other than in connection with a definitely related government procurement operation, the U. S. Government thereby incurs no responsibility, nor any obligation whatsoever; and the fact that the Government may have formulated, furnished, or in any way supplied the said drawings, specifications, or other data is not to be regarded by implication or otherwise as in any manner licensing the holder or any other person or corporation, or conveying any rights or permission to manufacture, use or sell any patented invention that may in any way be related thereto.

64-10

PB 181509

Price \$1.25

**AN INVESTIGATION OF MIDSHIP BENDING MOMENTS
EXPERIENCED IN EXTREME REGULAR WAVES BY
MODELS OF A TANKER AND A DESTROYER**

SSC-156

By

J. F. DALZELL

432182

SHIP STRUCTURE COMMITTEE

For sale by the U.S. Department of Commerce, Office of Technical Services,
Washington, D.C., 20230

CATALOGED BY DDC 432182
AS AD NO.

SHIP STRUCTURE COMMITTEE

MEMBER AGENCIES:

BUREAU OF SHIPS, DEPT. OF NAVY
MILITARY SEA TRANSPORTATION SERVICE, DEPT. OF NAVY
UNITED STATES COAST GUARD, TREASURY DEPT.
MARITIME ADMINISTRATION, DEPT. OF COMMERCE
AMERICAN BUREAU OF SHIPPING

ADDRESS CORRESPONDENCE TO:

SECRETARY
SHIP STRUCTURE COMMITTEE
U. S. COAST GUARD HEADQUARTERS
WASHINGTON 25, D. C.

3 February 1964

Dear Sir:

The Ship Structure Committee has sponsored a research project at Stevens Institute of Technology entitled "Model in Extreme Waves." The purpose of the project was to determine the upper limit of longitudinal seaway bending moments by direct measurement on ship models in tank waves of maximum steepness, supplemented by theoretical calculations.

Herewith is a copy of the Second Progress Report, SSC-156, An Investigation of Midship Bending Moments Experienced in Extreme Regular Waves by Models of a Tanker and a Destroyer by J. F. Dalzell.

The project was conducted under the advisory guidance of the Committee on Ship Structural Design of the National Academy of Sciences-National Research Council.

Comments on this report would be welcomed and should be addressed to the Secretary, Ship Structure Committee.

Yours sincerely,



T. J. FABIK
Rear Admiral, U. S. Coast Guard
Chairman, Ship Structure Committee

NATIONAL ACADEMY OF SCIENCES-NATIONAL RESEARCH COUNCIL

Division of Engineering & Industrial Research

SR-157 Project Advisory Committee
"Model in Extreme Waves"

for the

Ship Hull Research Committee

Chairman:

Mr. M. G. Forrest
Gibbs & Cox, Inc.

Members:

Mr. Harold Acker
Bethlehem Steel Co.

Mr. T. M. Buermann
Gibbs & Cox, Inc.

Professor C. Ridgely-Nevitt
Webb Institute of Naval Architecture

Professor W. J. Pierson, Jr.
New York University

SSC-156

Second Progress Report
of
Project SR-157
"Model in Extreme Waves"

to the

Ship Structure Committee

AN INVESTIGATION OF MIDSHIP BENDING MOMENTS
EXPERIENCED IN EXTREME REGULAR WAVES BY
MODELS OF A TANKER AND A DESTROYER

by

J. F. Dalzell

Stevens Institute of Technology

under

Department of the Navy
Bureau of Ships Contract NObs-78211

Washington, D. C.
U. S. Department of Commerce, Office of Technical Services
February 3, 1964

ABSTRACT

This report summarizes experimental research to investigate the possibility of a physical upper limit on midship bending moments in tanker and destroyer type ships being reached in regular waves of height significantly less than the theoretical upper limit of stability for progressive waves ($h/\lambda = 1/7$). Each model was tested at various speeds in regular head and following towing tank waves of several different lengths and of a wide range of heights. The results were compared with those obtained previously for a modern cargo vessel. No significant upper limit of bending moment was found. However, the study establishes more firmly the grossly linear dependence of midship bending moment on wave height, even for extreme wave heights which may be encountered in service. These findings strengthened the case for determining design wave bending moments on the basis of statistical analyses of ocean waves and/or resulting bending moments.

CONTENTS

| | <u>Page</u> |
|--|-------------|
| Introduction | 1 |
| Models | 2 |
| Description of Apparatus | 2 |
| Test Procedure and Program | 7 |
| Data Reduction | 10 |
| Test Results | 13 |
| A. Compilation | 13 |
| B. Condensation of Test Results | 14 |
| Analyses | 17 |
| A. Comparison with Other Test Data | 17 |
| B. Classification of Trends | 19 |
| C. Maximum Bending Moments in Waves of Fixed Height ... | 27 |
| D. Approximate Hydrodynamic Bending Moments | 28 |
| Discussion | 31 |
| A. Trends of Bending Moment with Wave Steepness | 31 |
| B. Trends of Motions Amplitudes with Wave Steepness | 32 |
| C. Results of Numerical Classification of Trends | 33 |
| D. Additional Confirmation of the Results of Section C | 34 |
| E. Bending Moments in Extreme Waves of Constant Height .. | 36 |
| F. Comparisons between Models | 36 |
| Conclusions | 36 |
| Recommendations | 37 |
| Acknowledgements | 37 |
| References | 37 |
| Nomenclature | 38 |
| Appendix | 40 |

NATIONAL ACADEMY OF SCIENCES-NATIONAL RESEARCH COUNCIL

Division of Engineering & Industrial Research

SR-157 Project Advisory Committee

"Model in Extreme Waves"

for the

Ship Hull Research Committee

Chairman:

Mr. M. G. Forrest
Gibbs & Cox, Inc.

Members:

Mr. Harold Acker
Bethlehem Steel Co.

Mr. T. M. Buermann
Gibbs & Cox, Inc.

Professor C. Ridgely-Nevitt
Webb Institute of Naval Architecture

Professor W. J. Pierson, Jr.
New York University

INTRODUCTION

Knowledge for design purposes of extreme wave bending moments on ship hulls in irregular storm seas is restricted to a relatively limited number of full-scale ship observations. Theoretical methods presently available for predicting hull bending moments in regular waves are also limited to prediction in moderate wave heights in which the effects are considered to be roughly linear. Efforts are currently being made toward determining design wave bending moments on the basis of statistical analyses of full-scale and model data, an approach which requires considerable expenditure of time and funds.

A possible alternate approach was detailed in Ref. 1 (Project 24) and a pilot study was made in the background work of that reference. This approach involved the possibility that an upper limit on midship bending moments might be found by the use of models in very steep tank waves. In the pilot study reported in Ref. 1, a model of a T-2 tanker was tested at zero and low speeds in head waves of model length and average heights ranging from $L/20$ to $L/8.5$. The measured midship bending moment amplitudes, plotted against local wave height, showed considerable scatter in the higher waves. Nevertheless, two tentative conclusions were drawn:

1. There appeared to be a tendency for the bending moment to fall off from a linear relationship with wave steepness as wave steepness was increased.
2. The highest recorded bending moments in head seas in the highest wave were between 10 and 20% greater than the results of conventional static $L/20$ calculation.

These conclusions suggested that reasonable maximum values of hull bending moments might be established experimentally by tests in very steep model tank waves. Project 24 of Ref. 1 entitled "Maximum Physically Possible Bending Loads," recommends such experiments and has as its objective: "To determine on a physical, rather than statistical, basis the upper limit of longitudinal seaway bending moments and shear forces expected on various ship types."

The present investigation stems from that recommendation and the basic philosophy was retained, which was to make a broad study of hull bending moments in regular waves of extreme steepness to see if the indications cited in the pilot study could be more generally applied. In this investigation, an attempt was made to cover as many of the known major variables as possible. Since data scatter in steeper waves was to be expected, it was felt that any parametric changes of the ship or of ship types should be as radical as possible so that differences would not be obscured.

The investigation was divided into two major parts. The first part was to consist of a study of one ship type and was to include investigations into the effects of variations in freeboard and weight distribution for that ship type. The second part of the project was to be a study of two additional different types of ship.

This report covers the second part of the investigation and deals with the experiments on two different ship types. The first part of the investigation is reported in Ref. 2.

MODELS

The choice of the Mariner as a trial horse in Ref. 2 was made on the basis of it being representative of good practice and a type likely to appear in quantity. The same philosophy was adopted in choosing the two models which, with the Mariner, were to comprise an investigation of the extreme bending moments measured in different ship types.

In recent years one of the most active segments of the ship building industry has been the tanker industry. Much published data are available on giant tankers and it was felt that one of the models chosen should be the largest and fullest tanker on which published data were available. Reference 3 shows a series of bulk carrier designs, the largest of which (Vessel J) is a 106,000 deadweight ton tanker. Vessel "J" of Ref. 3 was chosen as one of the models to be investigated. A reasonable weight distribution was derived for this model from published data. The characteristics of this model are given in the first column of Table I and Fig. 1 shows a model drawing. It can be noted in Fig. 1 that an instrument well was constructed amidships having fore and aft breakwaters extending 14.6% of LBP above the base line. As with the models reported on in Ref. 2, this well was necessary to prevent the model from flooding when great quantities of water washed over the decks. The model was made of wood, cut in half at Station 10, as indicated in the drawing, and completely decked over except for the top of the instrument well. It was necessary to put a "hat" over the forward part of the instrument well in order to keep spray from flooding the instruments.

Another ship type which fitted the criterion of representing good current practice, which was likely to appear in quantity, and which represented a large departure from the other models, was a destroyer. The particular destroyer chosen is described in Ref. 4. A model drawing is shown in Fig. 2. This model (2130) was outfitted with a simulated superstructure and gun mounts forward of Station 7. It was completely decked over except for an instrument well somewhat aft of midships, and contained its own bending moment balance. Coefficients and characteristics of this model are also shown in Table I. An approximate weight distribution was derived as for the tanker. A comparison of the weight distribution of the Tanker and Destroyer Models with that of the Mariner Model used in Ref. 2 is shown in Fig. 3. Because of the large amount of spray developed in the test of the destroyer model, and because of thin sheets of water running along the deck aft of the superstructure, the vertical front of the instrument well as shown in Fig. 2, was found to be insufficient to protect against spray coming into the model and a V-shape breakwater was added forward of the instrument well.

As is standard practice, the weight, centers and radii of gyration for each half of each model were calculated from the weight distribution (Fig. 3) and the models were ballasted to these figures. Natural pitching and heaving periods were obtained by manual oscillations in the wide tank, in accordance with standard techniques.

DESCRIPTION OF APPARATUS

Since the experiments on Models 2251D and 2130 were conducted immediately following those of Ref. 2, the test apparatus and techniques were the same. A schematic drawing of the mechanical test apparatus is given in Fig. 4. All models were attached to a towing apparatus which allowed freedom in pitching, heaving and surging motions, and restraint in yaw, sway, and surge. The apparatus permitted the model to be oriented bow towards the waves or away from the waves in DL Tank No. 3 (300'x12'x6'). This apparatus consists of a main carriage with an auxiliary rail and a sub-carriage to which is attached a vertical mast. The mast is restrained against all motions except vertical translation by ball bearing rollers. The sub-

TABLE I. MODEL CHARACTERISTICS.

| Model Number | 2251D | 2130 |
|-------------------------------------|--------------|----------------------|
| Design | Giant Tanker | Destroyer |
| Weight Distribution | Design | Design |
| Ship L.B.P., Feet | 895.0 | 383.0 |
| <u>MODEL CHARACTERISTICS</u> | | |
| Nominal Model Scale | 1:179 | 1:67.09 |
| Length on 20 Stations, inches | 60.00 | 68.5 |
| Beam, inches | 8.85 | 7.30 |
| Draft inches | 3.28 | 2.33 Fwd 2.68 Aft |
| Displacement, Pounds, F.W. | 52.0 | 25.1 |
| B/H | 2.70 | 2.92 |
| C_b | 0.80 | 0.55 |
| C_M | 0.99 | - |
| $\Delta/(L/100)^3$, Design | 172 | 62 |
| LCB, % Station Length From ∇ | 0.32 Fwd | 3.33 Aft |
| Gyradius, % Station Length | 22.7 | 23.4 |
| Natural Pitching Period, Sec. | 0.70 | 0.60 |
| Natural Heaving Period, Sec. | 0.80 | 0.65 |
| Natural Frequency of Vibration, CPS | 13.7 | 10.7 |
| Freeboards: Aft, inches | 1.56 | 1.37 |
| Fwd, inches | 2.52 | 3.44 |
| V.C.G., inches | 2.62 | 1.23 |
| <u>HALF MODEL, FWD SECTION</u> | | |
| Weight, lbs. | 26.6 | 11.2 |
| LCG Fwd ∇ , inches | 11.46 | 12.88 |
| VCG, inches | 2.60 | 1.06 |
| K_o , % Station Length/2 | 23.2 | 23.9 |
| <u>HALF MODEL, AFT SECTION</u> | | |
| Weight, lbs. | 25.4 | 13.9 |
| LCG Aft ∇ , inches | 11.59 | 14.56 |
| VCG, inches | 2.65 | 1.37 |
| K_o , % Station Length/2 | 25.2 | 25.6 |

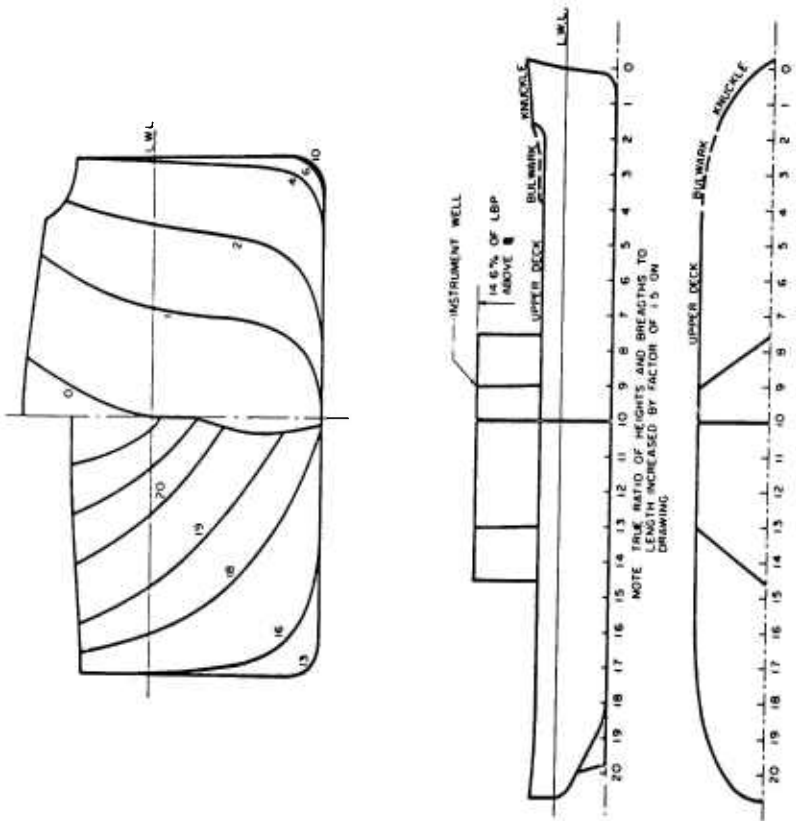


FIG. 1. MODEL DRAWING, MODEL 2251D, GIANT TANKER.

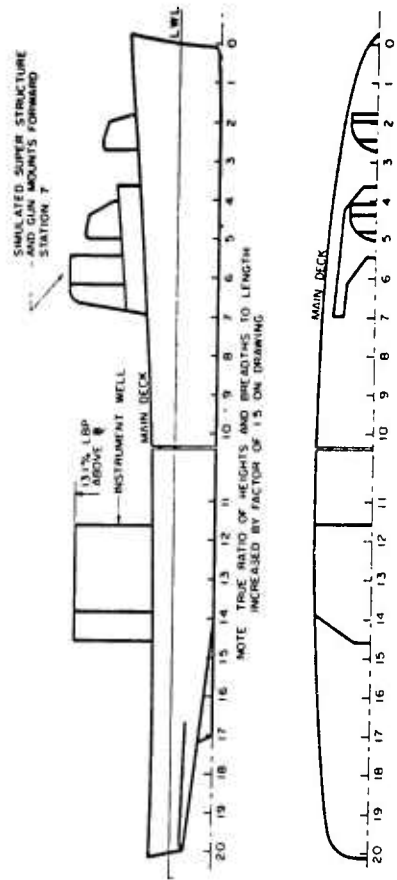
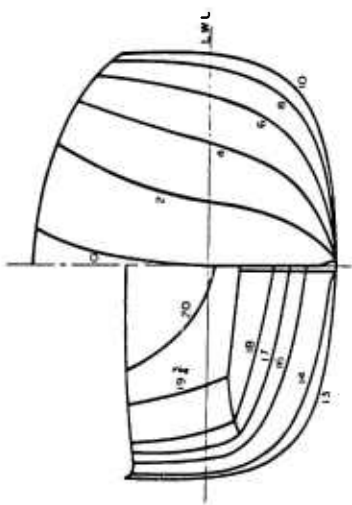


FIG. 2. MODEL DRAWING, MODEL 2130, DESTROYER.

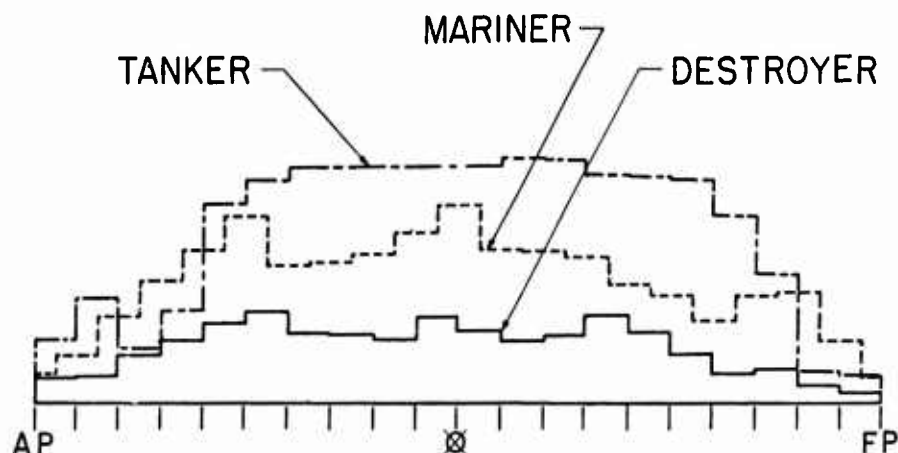


FIG. 3. WEIGHT DISTRIBUTIONS.

carriage carrying the vertical mast is itself restrained against all motion except fore and aft translation. The model is attached to the bottom of the mast by pivots with axis athwartships, thus allowing freedom in pitch and restraining rolling motion.

A gravity weight towing system was employed, Fig. 4, in which a falling weight provided a force between the main and the sub carriages. This force was transmitted through the pitch pivots to the model and caused the model and subcarriage to move, resulting in a change in the relative distance between the subcarriage and main carriage. This distance was measured and used as an error signal in a servo system which controlled the main carriage so as to minimize changes in relative position of main and sub carriages. If forward speed was required, a towing force was applied to the model from the falling weight system, the model then proceeded at whatever speed it would, and the main carriage followed. Tow forces could be applied in either direction. Since this method provided no means of accelerating the model, the model was accelerated by hand from the starting position. After the model reached the end of the run the towing weight was electrically dropped out and the model then slowed down of its own accord. The recording run length was about four model lengths for runs in which the model moved at speed. The elapsed time from one end of this run area to the other was measured in order to derive average model speed. In addition, in most of the runs, a continuous record of model speed was obtained by a tachometer and roller fixed between the model subcarriage and the main tank rail.

Heaving and pitching motions were measured by potentiometers attached to the vertical mast and to the pivots in the model. Because of the heavy concentrated instrumentation loads in the models it was not possible to satisfy simultaneously the ballasting requirement and the requirement that the heaving motion be measured at the center of gravity. Therefore the pitch pivot was located between six and eight inches aft of the LCG depending on the model, and an electronic circuit was devised to correct the resulting heave transducer signal from "heave at the pitch pivot" to "heave at the LCG." This correction was made in a linear fashion in accordance with the following equation:

$$z_{LCG} = z_{pp} + a \theta, \text{ where } a \text{ is the distance from pitch pivot to LCG}$$

Wave elevations were measured with a resistance type wave probe, two feet long, and designed for use in a plus or minus six inch range. Linearity of the probe was within one percent of the full scale range. The wave probe was located approximately five feet ahead of amidships on the model.

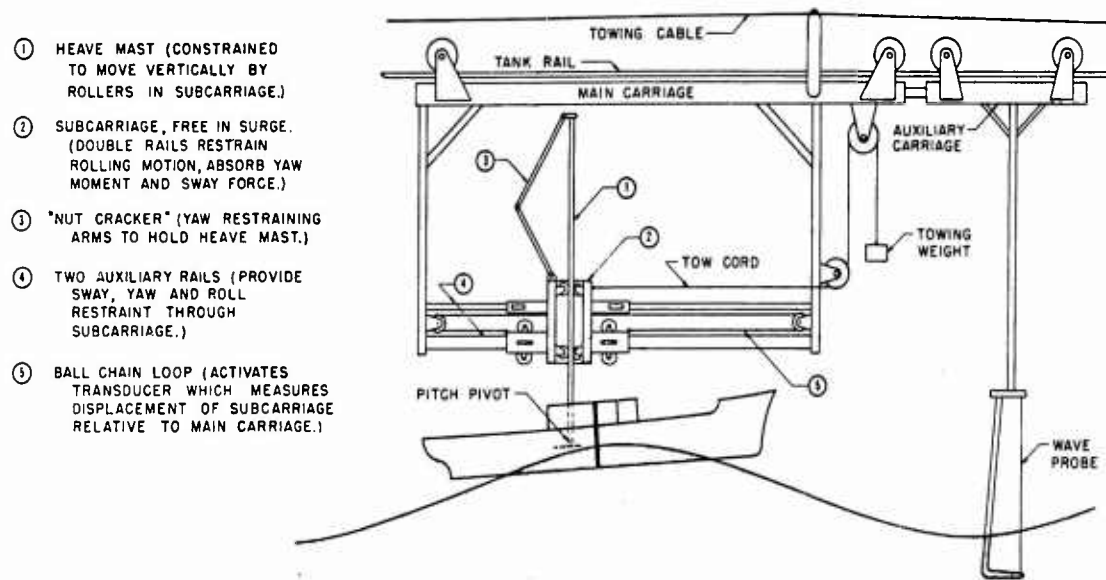


FIG. 4. SCHEMATIC OF TOWING APPARATUS.

Model 2130 (the destroyer) was outfitted with its own bending moment balance. A description of this balance may be found in Ref. 4. The bending moment balance described in Ref. 2 was used for Model 2251D. A drawing of a bending moment instrumentation installation almost the same as that for Model 2251D is shown in Fig. 5. While the detail in this drawing does not apply to the destroyer instrumentation, the general scheme is identical. In both cases the two halves of the model were connected by an aluminum beam about six inches long. The relative angular deflections at both ends of the beam were measured by differential transformers and these were connected so as to yield a signal proportional to pure bending deflection of the beam. The joint between the two halves of the model was sealed by a thin rubber bellows (Fig. 5). The natural frequencies of vibration in water of both models are given in Table I. Calibration of the balances was done with the models in the water by applying couples equal and opposite to the forward and after part of the model and recording the resulting signals.

To summarize: The instrumentation was arranged so that signals proportional to midship bending moment, pitching motion, wave elevation up-wave from the model, and speed were available. These signals were recorded on a standard carrier amplifier-oscillograph system. The same electronic filter was used to filter the signals from the bending moment balances as was used in Ref. 2, and (as in that reference) the net frequency response of the bending moment measuring system was calculated and is shown in Fig. 6 in this report. The results for Model 2251A-VI, the parent Mariner model of Ref. 2 are also shown in Fig. 6. Model 2130, the Destroyer Model, has a resonance peak at much lower frequency than the models built under this project because of the different balance used. The maximum frequency range of interest is shown in Fig. 6 and while corrections to the bending moment data were made in this range, it is seen that by and large they are not highly significant. The transient response to half sine-wave impulses were also derived in the same manner as in Ref. 2 and the results are shown in Fig. 7. Just as in that reference, it can be seen that output pulse widths shown on the oscillograph, whose width at the midheight is greater than 0.15 sec., represent a good measurement of the phenomena. A loss in accuracy can be expected of the order of from one to twenty percent for apparent pulse widths ranging between 0.1 and 0.15 seconds. It can be seen that the Destroyer Model bending moment system has a larger range of pulse widths where good resolution is to be ex-

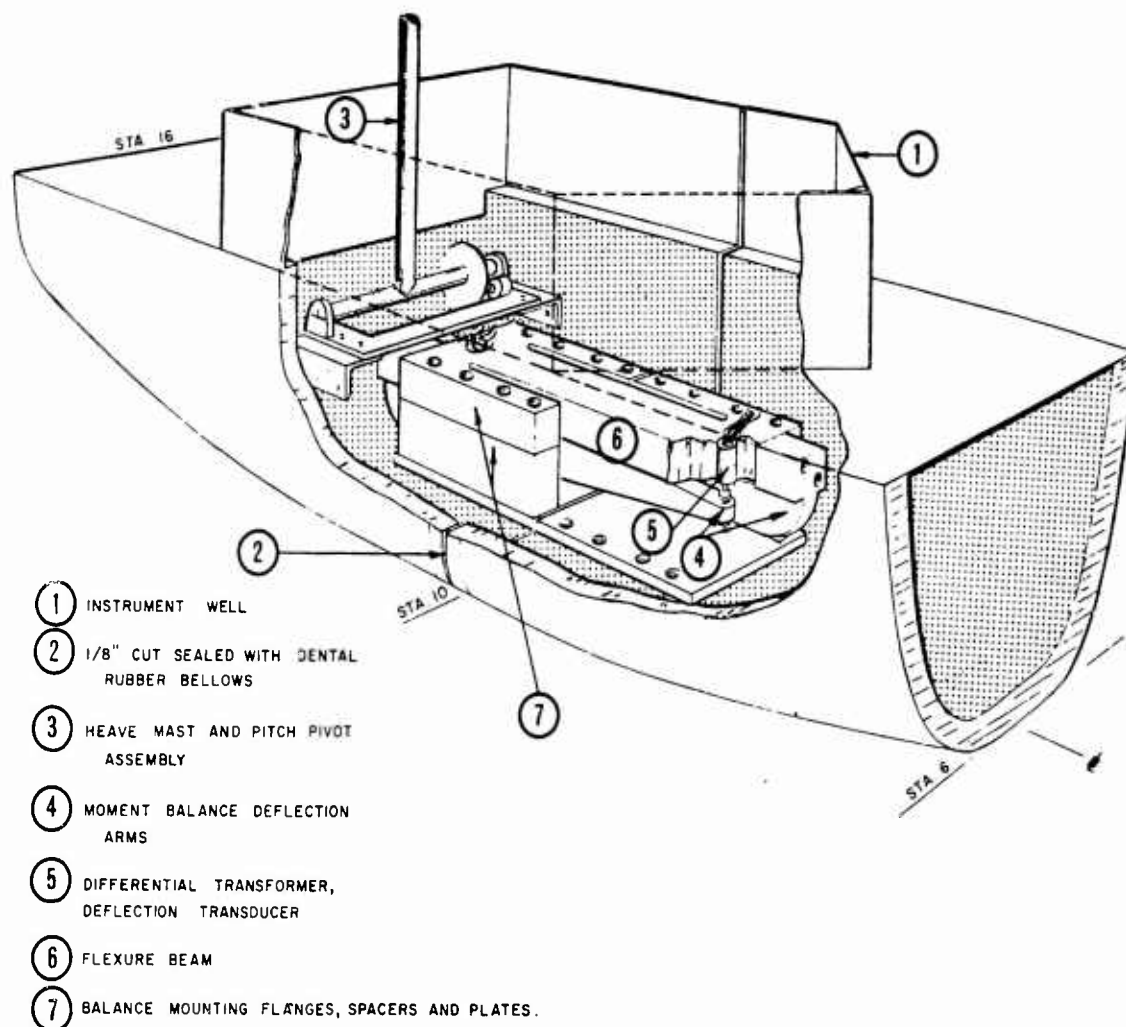


FIG. 5. ARRANGEMENT OF INSTRUMENTATION IN A TYPICAL MODEL.

pected. As in Ref. 2 suppression of the impulsive moment due to loads acting over very short periods of time is to be expected.

TEST PROCEDURE AND PROGRAM

After calibrating each item to be measured, electrical check signals were put on about every third record taken (to expose any electronic drifts in the system), and closing calibrations were usually carried out at the end of the testing day. Static calibration factors remained steady over a period of two or three test days. Calibration constant differences due to sensitivity drifts in the electronic apparatus were seldom more than 3% over such a period.

For each run the wavemaker was started and, in the case of a run at speed, the model was accelerated by hand when the test area (a 100-foot length of DL Tank No. 3 adjacent to the wavemaker) was filled with waves. Because the towing apparatus was servo operated, the model attained a more or less constant speed and would proceed up (or down) the tank through the run area. The elapsed time it took the model to traverse the run area was recorded and an oscillograph record was made of all the measurements while the model was in the run area. After the model proceeded out of the run area, the oscillograph was stopped and the towing weights were dropped off to slow the model down and eventually stop it. For tests at zero speed, it was found neces-

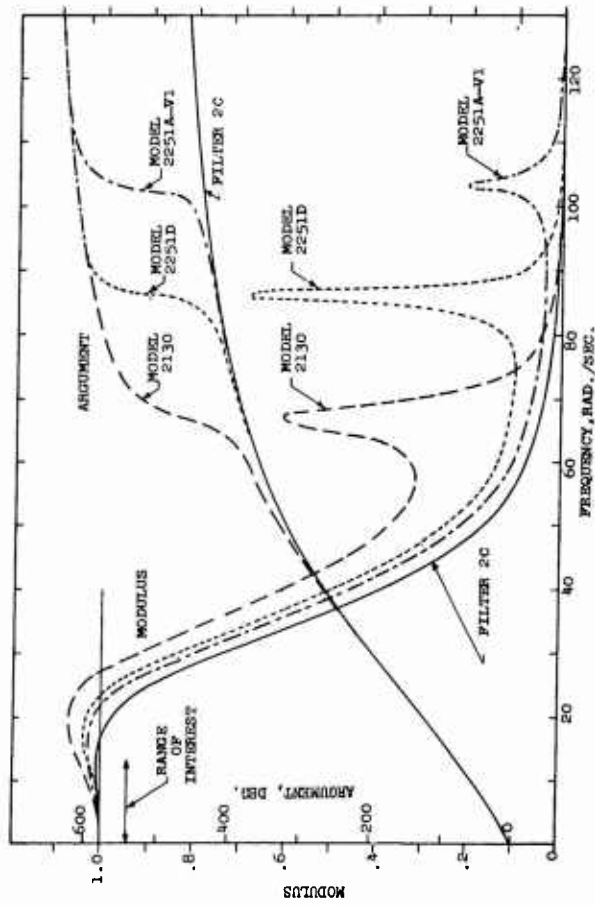


FIG. 6. FREQUENCY RESPONSE OF BENDING MOMENT MEASURING SYSTEM.

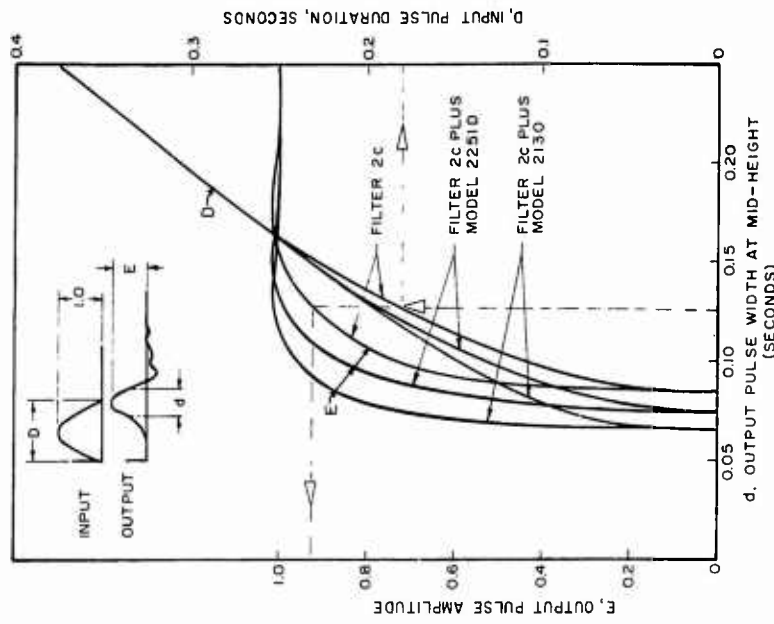


FIG. 7. TRANSIENT RESPONSE OF BENDING MOMENT MEASURING SYSTEM TO HALF-SINE PULSES.

TABLE II. TEST PROGRAM - GIANT TANKER AND DESTROYER MODELS.

| Model 2251D | | GIANT TANKER | | | | | |
|-------------|-------------------|--------------------------|-----|------|------|------|------|
| Heading | Speed Classif. | Wave Length/Model Length | | | | | |
| | | .50 | .75 | 1.00 | 1.25 | 1.50 | 1.75 |
| 180° | Zero | 4 | 5* | 6* | 6* | 6* | 4* |
| " | Forward | 4 | 4 | 5 | 5* | 5 | 4 |
| " | Drifting | | 4 | 5 | 5* | 5 | 4 |
| 0° | Zero | | | 5 | 5 | 5 | |
| " | Forward | | | 5 | 5 | 5 | |

| Model 2130 | | DESTROYER | | | | | |
|------------|-------------------|--------------------------|-----|------|------|------|------|
| Heading | Speed Classif. | Wave Length/Model Length | | | | | |
| | | .50 | .75 | 1.00 | 1.25 | 1.50 | 1.75 |
| 180° | Zero | | 4* | 5* | 5* | 5* | 4* |
| " | Forward | | 4 | 5 | 5* | 5 | 4 |
| " | Drifting | | 4 | 5 | 5* | 5 | 4 |
| 0° | Zero | | | 5 | 5 | 5 | |
| " | Forward | | | 5 | 5 | 5 | |

- a. Numbers in the blocks indicate the number of good runs obtained in order to cover the range of wave height. Blanks indicate no runs attempted.
- b. * Indicates a motion picture record of the model in the highest wave.

sary to bypass the servo drive and to allow the towing weights and extremely weak springs to govern the relative motion between the model subcarriage and the stationary main carriage. In this condition the model was located in the middle of the test area.

The preliminary test work of Ref. 2 had resulted in a standardized test program which was followed in the present work for both models. This test program, which is detailed in Table II, involves tests in waves of from 0.75 to 1.75 times the model length at five speed and heading combinations. Three head sea speeds were examined, one at zero speed, one at a standard Froude number between 0.12 and 0.14, and one at a negative speed which was dictated, in each wave length, by the drifting speed naturally attained by the model in the highest wave generated. Two following sea cases were examined, zero speed and a forward speed corresponding to about twice the drifting speed. The numbers entered in Table II indicate the number of runs obtained in order to cover the possible range of wave heights for each wave length at each speed.

Since no prior experience had been had with bending moments in giant tankers, runs in a wave length of 0.50L were added. Extensive data were available on the Destroyer Model in moderate waves (Ref. 4 and 5) and it was felt that the wave length range in the standard program was adequate.

As in Ref. 2, motion pictures were taken of the models at zero speed in head seas of five wave lengths and at the forward speed and the drifting astern speed in the 1.25L wave length.

DATA REDUCTION

It was decided to assess the magnitudes of moments and motions in waves by measuring the maximum and minimum of each cycle of the time histories obtained. For the waves and the pitch and heave motions, the sums of the maxima and minima were measured and tabulated (double amplitudes). For the bending moments the maxima and the minima (sag and hog) of the filtered bending moment trace were measured. This was done for as many cycles as possible up to a maximum total of 20. In the zero speed cases, between 16 and 25 cycles were recorded and up to 20 were measured and tabulated. Because of the instability of the waves and the variation in height from cycle to cycle the average of the maxima, minima, and double amplitudes were calculated as were the root mean square deviations of these measurements from their respective means. The averages were used thereafter as test points. Most of the data handling after the initial measuring of the oscillograph traces was done on an IBM 1620 Computer.

All data were non-dimensionalized as much as possible in the course of the data reduction. Wave steepness was expressed as wave height to length ratio, h/λ , wave length was expressed as the wave length to ship length ratio, λ/L . The symbol 2θ stands for the double amplitude of pitch in degrees. The heaving double amplitude was divided by the model length to present heave results ($2Z_o/L$).

All bending moment amplitudes were converted to a non-dimensional coefficient form. The form selected was the bending moment (hog or sag) divided by the quantity $\rho g L^3 B$ where ρg is the weight density of water, L is the model length, B is the maximum model beam. The coefficient normally used to express results from tests in moderate waves is similar but contains the wave height in the denominator. The two coefficients are related as follows:

If μ = moment coefficient used herein

and C = moment coefficient used in moderate wave tests

M = bending moment

$$\mu = \frac{M}{\rho g L^3 B}, \quad C = \frac{M}{\rho g L^2 B h}$$

$$\text{Then } \mu = C \cdot (h/\lambda) \cdot (\lambda/L)$$

Preliminary data reduction and presentation of Ref. 2 indicated that presentation of individual test points on charts where more than one wave length was included were confusing. It was felt that final conclusions would depend heavily on the lines faired through the test data, and that interpretation would depend to a great extent on the adequacy of fairing of mean lines through the test spots. Since some degree of subjectivity in fairing data was inevitable, it was decided to concentrate the subjectivity into the form of an equation to be fitted impartially to each set of data by the IBM 1620 Computer. The data was sorted into test groups each of which contained the data for all the various wave heights obtained for a particular model, speed, heading and wave length. A curve was fitted to each of the resulting plots of average sagging moment, hogging moment and pitching and heaving amplitude vs. wave steepness. The form of the equation was as follows:

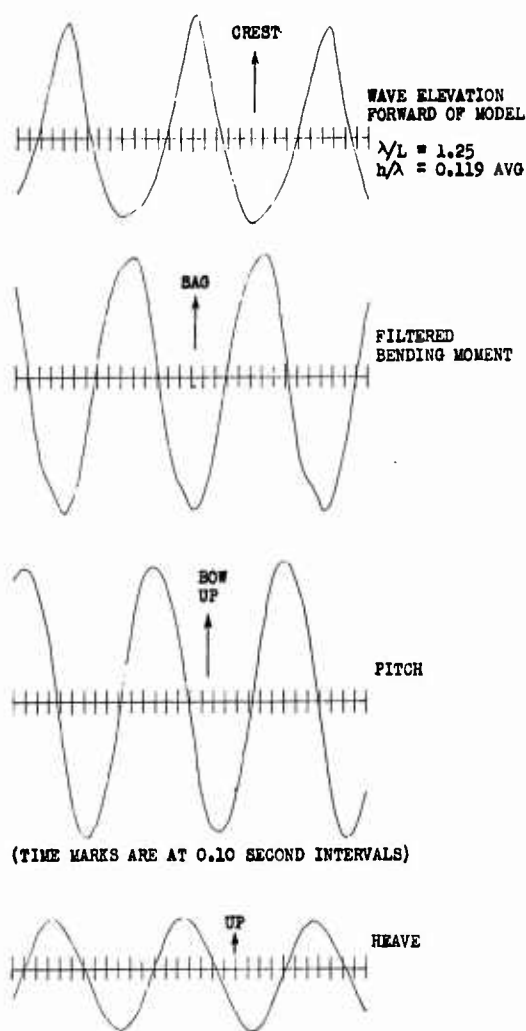


FIG. 8. SAMPLE OSCILLOGRAPH TRACING:
 RUN 716, MODEL 2251D, GIANT TANKER,
 HEAD SEAS, ZERO SPEED.

$$Y = a(h/\lambda) + b(h/\lambda)^N$$

Where: Y = bending moment, pitch or heave amplitude
 h/λ = wave steepness
 a, b = coefficients
 $N = 2, 3$ or 4

The computer actually fitted three such equations, one for each value of N , for each response and chose the best fit on the basis of the least residual mean square deviation from the test data. It then evaluated the resulting equation for values of h/λ convenient in plotting. The resulting fitted lines were judged to be of the form which would have resulted from hand fairing. No great significance is attached to the values of the coefficients obtained. The procedure followed was merely to insure consistency of method rather than to provide material for generalization. A two-term equation was selected to avoid over-fitting the test spots, on the basis of preliminary fitting with three and four term equations.

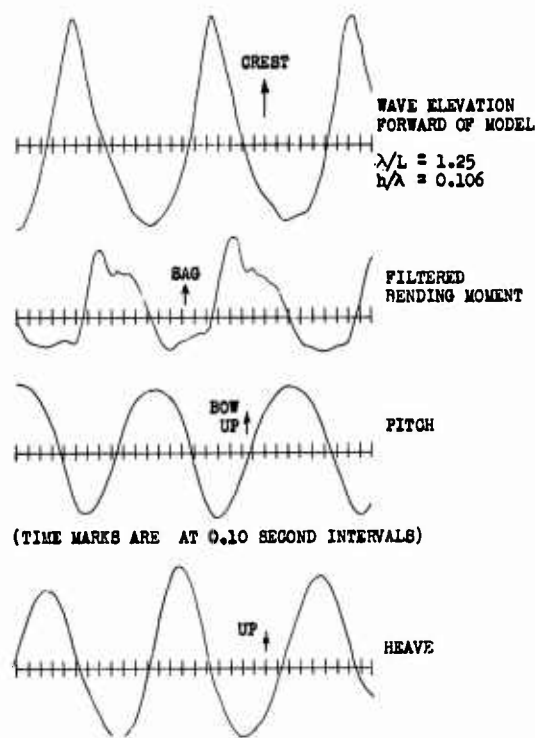


FIG. 9. SAMPLE OSCILLOGRAPH TRACING:
 RUN 1022, MODEL 2130, DESTROYER,
 HEAD SEAS, ZERO SPEED.

MODEL 2251D TEST GROUP 1,401150
 WAVE LENGTH: 1.50 L MODEL HEADING: 180°
 APPROX MODEL SPEED: $v/\sqrt{gL} =$ 0.0

TABLE III. SAMPLE DATA TABULATION.

| | | | | | | |
|--|----------------|------------|----------------------------------|----------|-------|-------|
| Model: <u>2251D - Giant Tanker</u> | | | Test Group: <u>1,401150</u> | | | |
| Zero Wave Bending Moment Corresponds to a Still Water Moment of: <u>0,000h⁵ SAG</u> | | | Wave Length: <u>1,50</u> L | | | |
| 1.0L Static Calculations (Non-Dimensional) | | | Heading: <u>180</u> Degrees | | | |
| Wave Height | Wave Sag | Wave Hog | Speed: <u>0,0</u> | | | |
| <u>L/20</u> | <u>0,0007h</u> | <u>---</u> | Heave Tuning Factor: <u>0,65</u> | | | |
| Bow-up-Pitch Lags Sagging Moment Approx.: <u>105</u> Degrees | | | Pitch Tuning Factor: <u>0,60</u> | | | |
| Up-Heave Lags Sagging Moment Approx.: <u>180</u> Degrees | | | | | | |
| Coefficients of Equation Fitted to Run Averages of Amplitude | | | | | | |
| Y = | μ_s | μ_H | μ_θ | $2Z_0/L$ | | |
| N | 2 | 2 | 2 | 4 | | |
| a | .0180 | .0157 | .256 | .734 | | |
| b | -.0741 | -.0327 | .127 | .187 | | |
| RMS Deviations of Measured Amplitudes within Each Run (Units consistent with those on plot) | | | | | | |
| Run No. | 754 | 771 | 776 | 784 | 787 | 791 |
| h/λ | .0927 | .0867 | .0789 | .0670 | .0472 | .0983 |
| No. Cycles | 16 | 16 | 16 | 16 | 16 | 16 |
| rms Wave x 10 ² | .21 | .22 | .25 | .08 | .14 | .18 |
| rms Sag x 10 ⁴ | .30 | .19 | .27 | .14 | .19 | .32 |
| rms Hog x 10 ⁴ | .20 | .11 | .36 | .14 | .14 | .20 |
| rms Pitch, deg. | .66 | .38 | .57 | .34 | .30 | .29 |
| rms Heave x 10 ² | .25 | .20 | .28 | .17 | .19 | .13 |
| REMARKS: (1) Form of Equation: $Y = a(h/\lambda) + b(h/\lambda)^N$ | | | | | | |
| (2) | | | | | | |

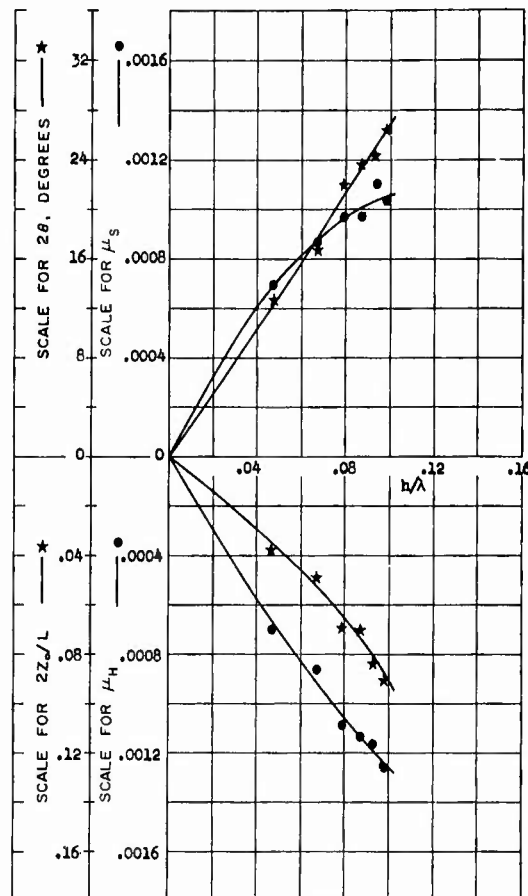


FIG. 10. SAMPLE BASIC DATA CHART.

As in Ref. 2, approximate phase relations between pitch, heave and bending moment were estimated. The results were of the same magnitude as those for the models reported in Ref. 2, and the values reported herein are averages over all models (including those of Ref. 2) and wave heights at the same wave length and speed.

Figures 8 and 9 show tracings of short sections of oscillograph records from one of the tests of Model 2251D, the Giant Tanker, and from one of the tests of the Destroyer model (2130). It can be seen in Fig. 9 that the filtered bending moment trace is far from sinusoidal. The top of the initial sagging hump was taken as the maximum sagging moment in the data reduction process. An examination of the first superimposed hump on the sagging moment trace of Fig. 9 shows that the pulse width at midheight is about 0.1 sec. and thus (see Fig. 7) the indicated maximum is probably in error less than 5%. As near as can be told from the motions records, this hump occurred when the bow submerged into the oncoming wave. A bottom impact should have occurred before the superimposed sagging moment hump, but the effect of any sharp impact has apparently been lost in the response of the measuring system.

All test records were examined taking into account the data in Fig. 7, and it was concluded that distortion of the maximum wave moments was not very great. Instances were noted where the bending moment traces resemble those in Fig. 9 rather than those in Fig. 8.

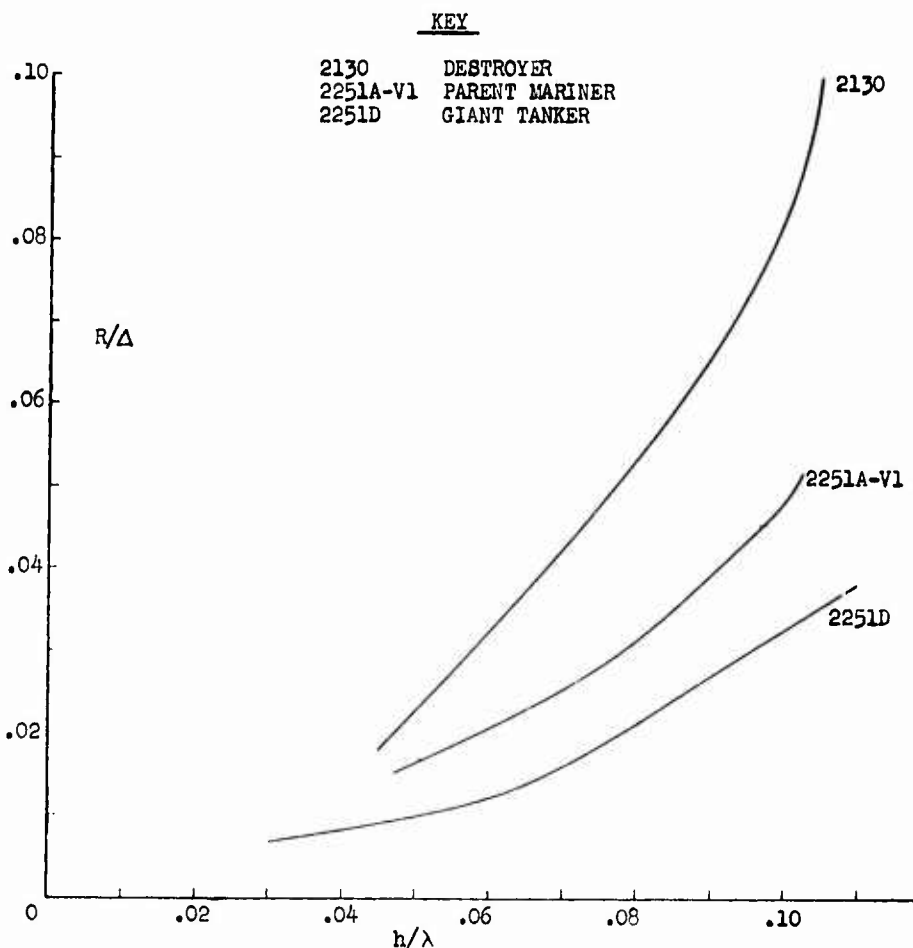


FIG. 11. UPPER ENVELOPE OF MODEL RESISTANCE IN WAVES OF ALL LENGTHS, HEAD SEAS, FR. NO. = 0.12 to 0.14.

TEST RESULTS

A. Compilation

Test results were grouped in accordance with the blocks in the test program of Table II, that is, all data obtained in the same wave length, heading, speed and for the same model were grouped together. All basic test data are contained in Ref. 6, and because all the data consumes 76 pages of that reference only a sample is presented herein. The data for each test group was summarized in two pages, one of which is a chart, the other a tabulation. Table III is a sample data tabulation, Fig. 10 the corresponding sample chart.

The chart, Fig. 10, shows the test spots and the fitted lines for the bending moment and motion amplitudes. Test spots for moments are shown as circles, those for motions are stars. All amplitudes are plotted to a base of wave steepness. The variability of the wave height measurement in the most severe wave was made the criterion by which the fitted curves were said to represent the test range of h/λ . The lines fitted to the amplitude data were extended in each case to a wave steepness corresponding to the average wave steepness observed in the most severe wave plus one and a half times the root mean square deviation of the wave height measurements in that run. This procedure reflects the significant range of scatter of individual wave amplitudes.

The supporting tabulation, Table III, in addition to indicating the model number, description, wave length, heading and speed, shows the heave and pitch tuning factors which are the ratios of the frequency of encounter to the natural frequencies of oscillation. The tabulation also shows the results of standard static calculations. These results are separated into still water moment and wave moments. The still water bending moments were obtained by calculations based on the hydrostatic properties of the model and the model ballasting results. The standard static wave moment calculations shown do not include Smith effect. A static L/20 hogging moment calculation was not available for the Giant Tanker, Model 2251D.

The tabulation, Table III, also gives the approximate motion phase lags and the coefficients of the equations fitted to the average measured amplitudes. There follows a tabulation of the run numbers, the approximate average wave steepness measured, the number of cycles analyzed and the root mean square deviations of the measurements within each run. Where applicable, remarks were made in the tabulations pertaining to the existence of bottom impacts. These represent opinions formed during a check of the tape records against the applicable transient response curves of Fig. 7.

An analysis was made of the forces necessary to tow the models in head seas at the forward speed Froude number of 0.12 to 0.14. The upper envelope of all results are shown for both models in Fig. 11, where tow forces per unit displacement are plotted against wave steepness. Corresponding data for the Mariner type ship from Ref. 2 is also included in Fig. 11.

On the basis of analyses in Ref. 2, it was assumed that the trends of moments in head and following seas would be much the same. Therefore, analysis of following sea, zero speed data was not made for the tests of the two models described herein.

B. Condensation of Test Results

1. Trends of Bending Moment with Wave Steepness.

To simplify correlation and comparison the faired lines through the data applicable to each model (Ref. 6) in each speed-heading condition have been plotted together in Figs. 12 through 19. These figures are arranged in the following order:

- 12-13 Both Models, Head Seas, Forward Speed
- 14-15 Both Models, Head Seas, Zero Speed
- 16-17 Both Models, Head Seas, Drifting Astern
- 18-19 Both Models, Following Seas, Forward Speed

Scales are the same in all figures. Wave steepness (h/λ) is the abscissa, bending moment coefficient the ordinate. The vertical scale at the left on the plot denotes wave hogging and sagging moments (μ , μ_H). The scale to the right on each plot is the "absolute" bending coefficient (μ_{HA} , μ_{SA}); that is, the origin of the wave bending coefficient scale has been translated to account for the static still water bending moment. This scale corresponds to the bending moments ordinarily obtained in the design office. The results of conventional static calculations in model length waves are shown where available. The numbers which label each of the lines drawn on these plots indicate the wave length to ship length ratio.

2. Trends of Pitch and Heave Amplitudes with Wave Steepness.

A condensation similar to that for bending moments has been made of the faired lines through the pitch and heave amplitude data (Ref. 6). This condensation is shown in Figs. 20 to 27 which are arranged in the following order:

MODEL 2251D, GIANT TANKER
 MODEL HEADING: 180° HEAD SEAS
 APPROX. MODEL SPEED: $v/\sqrt{gL} = 0.12$ to 0.14

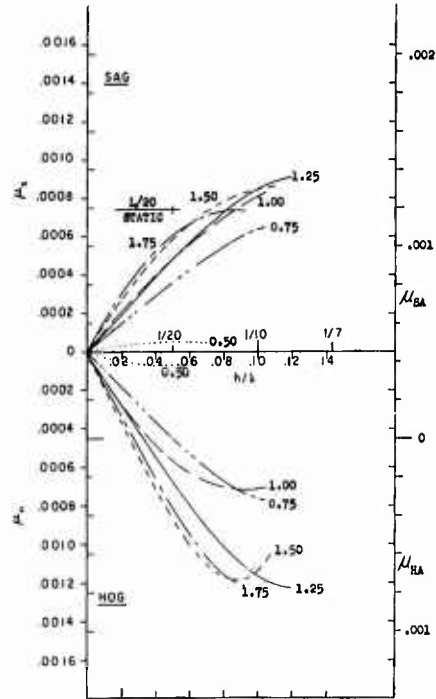


FIG. 12.

MODEL 2130, DESTROYER
 MODEL HEADING: 180° HEAD SEAS
 APPROX. MODEL SPEED: $v/\sqrt{gL} = 0.12$ to 0.14

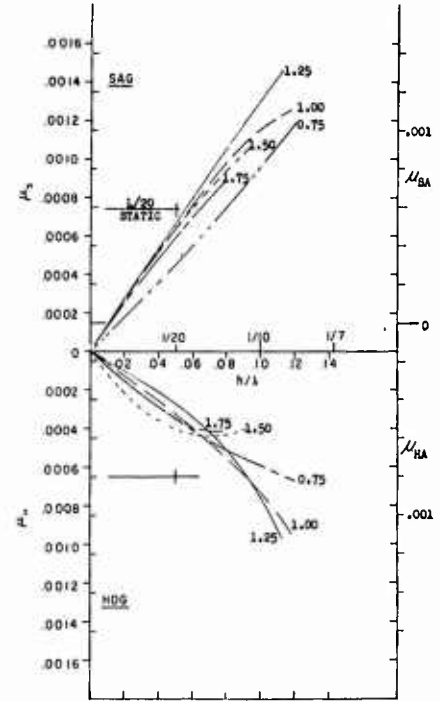


FIG. 13.

MODEL 2251D, GIANT TANKER
 MODEL HEADING: 180° HEAD SEAS
 APPROX. MODEL SPEED: $v/\sqrt{gL} = 0.0$

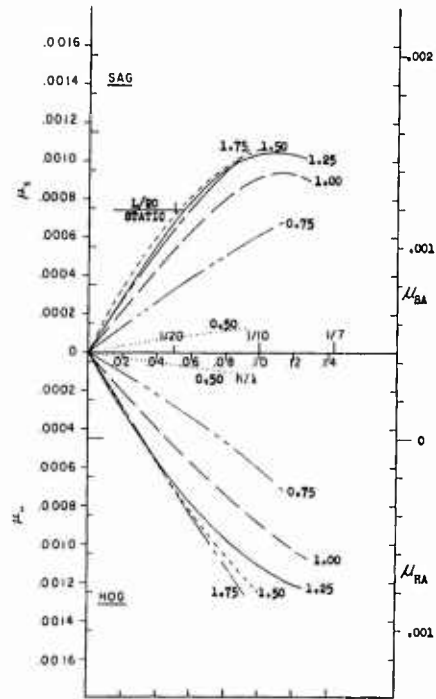


FIG. 14.

MODEL 2130, DESTROYER
 MODEL HEADING: 180° HEAD SEAS
 APPROX. MODEL SPEED: $v/\sqrt{gL} = 0.0$

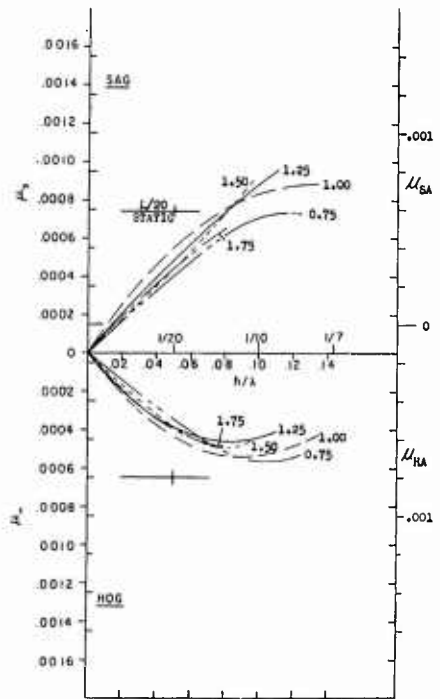


FIG. 15.

FIG. 12-15. TRENDS OF BENDING MOMENT WITH WAVE STEEPNESS.

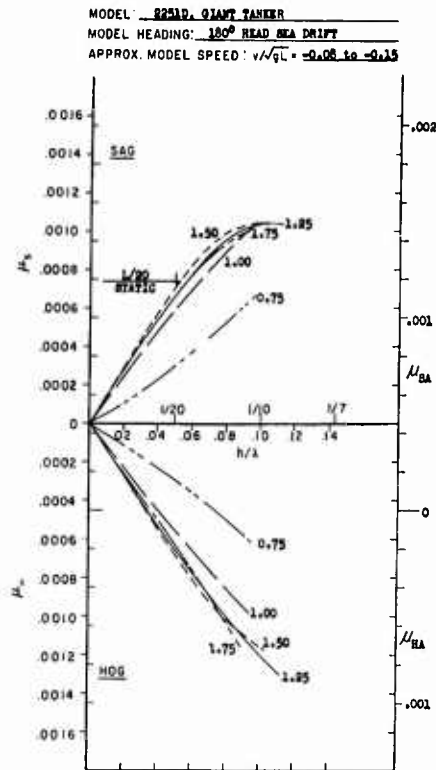


FIG. 16.

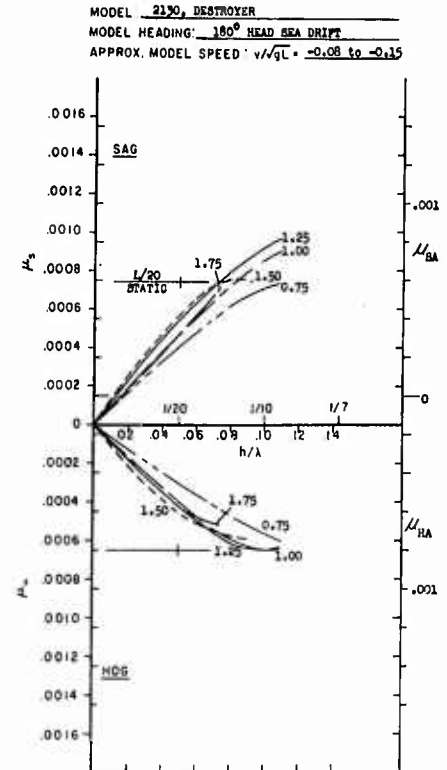


FIG. 17.

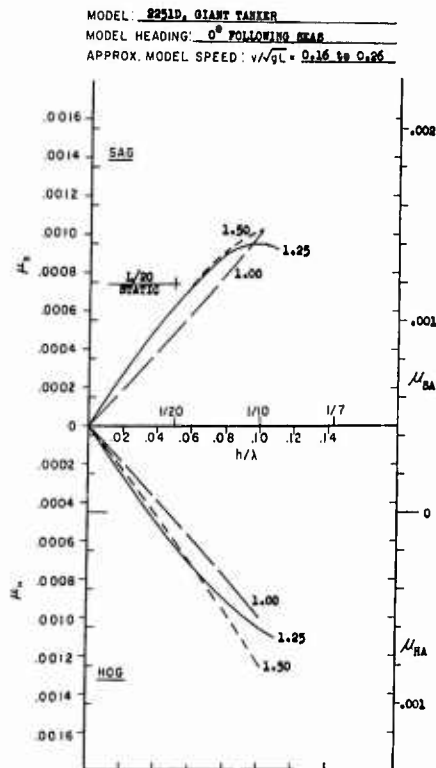


FIG. 18.

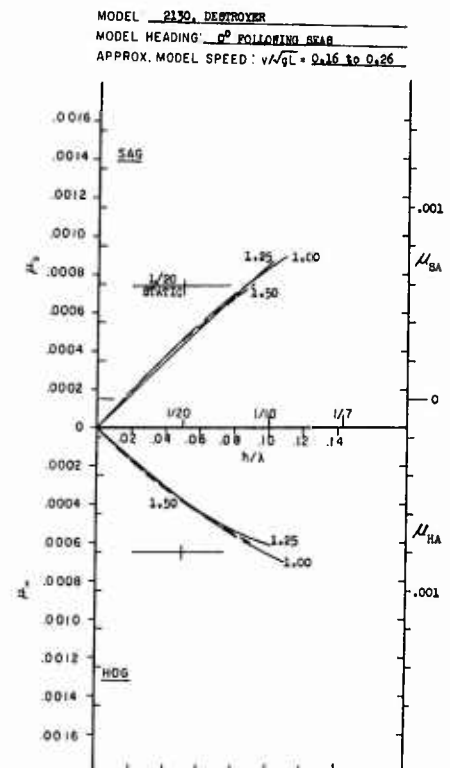


FIG. 19.

FIG. 16-19. TRENDS OF BENDING MOMENT WITH WAVE STEEPNESS.

- 20-21 Both Models, Head Seas, Forward Speed
- 22-23 Both Models, Head Seas, Zero Speed
- 24-25 Both Models, Head Seas, Drifting Astern
- 26-27 Both Models, Following Seas, Forward Speed

Scales are the same in all figures. The top half of each is a plot of pitch double amplitude in degrees (2θ) against wave steepness and the bottom half is a similar plot of heaving amplitudes ($2Z_0/L$). Lines are labeled with the applicable wave length to ship length ratio.

3. Cross Plots of Bending Moments and Motions.

In order to facilitate comparison between models, cross plots were made of the data in Figs. 12 to 27 for wave steepnesses of 0.04 and 0.10. The resulting plots are presented in Figs. 28 to 31. Cross-plotted moments and motions are shown for the various speed cases as follows:

- Figure 28 Head Seas, Forward Speed
- " 29 Head Seas, Zero Speed
- " 30 Head Seas, Drifting Astern
- " 31 Following Seas, Forward Speed

At the upper left hand side of each figure, cross plots of pitching amplitudes at the two wave steepnesses are shown. Heaving double amplitudes are cross-plotted in similar fashion directly below. The next plot, from left to right on each figure, shows wave sagging and hogging moments for wave steepness of 0.04. The plot immediately adjacent is of sagging and hogging moments at a wave steepness of 0.10. The plot at the far right of each figure in which the ordinate is labeled u'_S and u'_H , is of approximate hydrodynamic bending moments. The source of these "hydrodynamic" bending moments will be discussed subsequently.

The abscissa of each plot is wave length to ship length ratio, and notation is the same as in Figs. 12 to 27. Arrows shown at the ends of some of the lines show the direction in which the line would go if the point on the faired curve for the next higher wave length had been plotted. In all cases where an arrow is shown the faired line through the data points for the next higher wave length did not extend to a steepness of 0.09 and was therefore not considered valid for a wave steepness of 0.10.

Line conventions denoting the models are shown on each plot. Similar data from Ref. 2 pertaining to the Parent Mariner model has also been included in the cross plots.

ANALYSES

A. Comparison with Other Test Data

A question which is frequently raised is that while data presented may be consistent with itself, the possibility exists that it may not be consistent with previous data. In order to make a comparison with previous data, attention must be concentrated on results in waves of a steepness below 0.05 ($\lambda/20$). In the present work very little data were obtained in this region, but it is of interest to compare the mean slope of the fitted curves in the very low wave height region with previously obtained data. The slope of the fitted curves in this region may be used to obtain the moment coefficient ordinarily used in the presentation of bending moment data in moderate waves. That is:

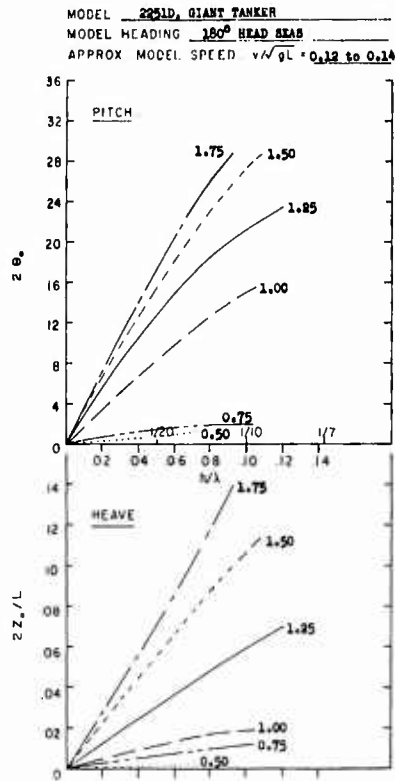


FIG. 20.

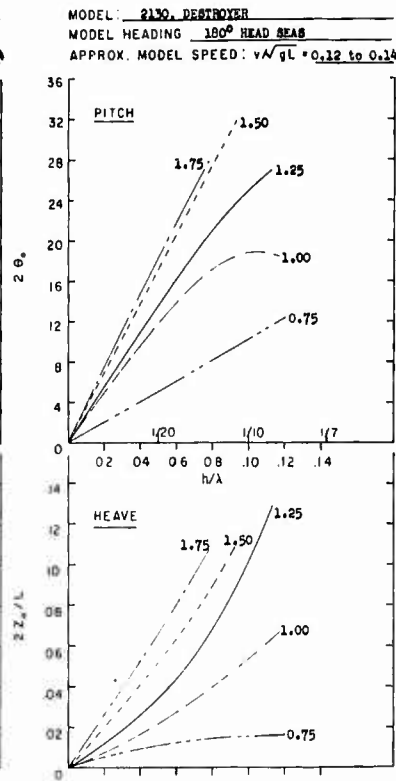


FIG. 21.

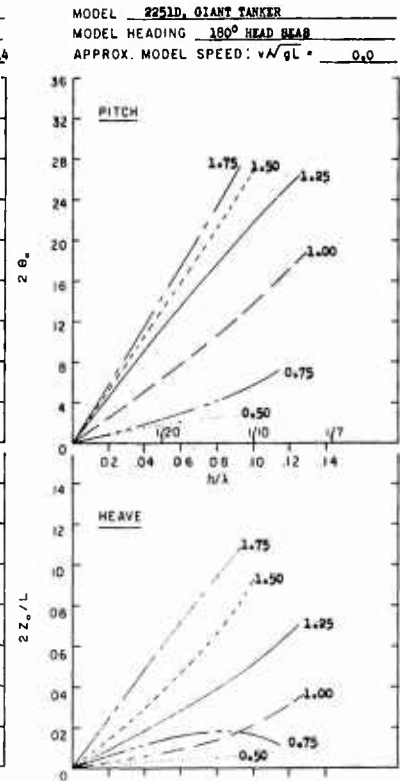


FIG. 22.

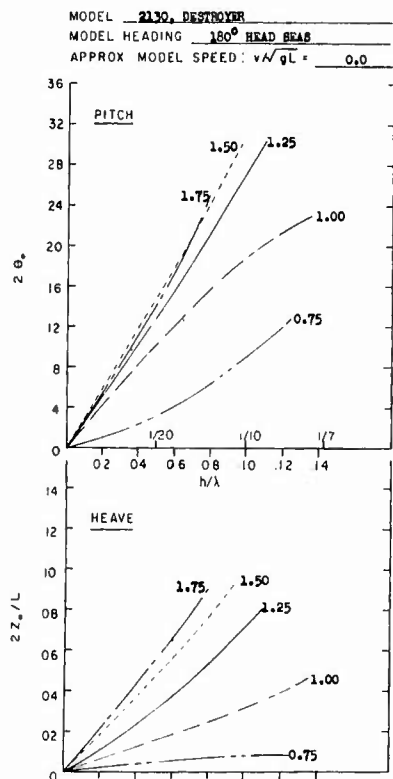


FIG. 23.

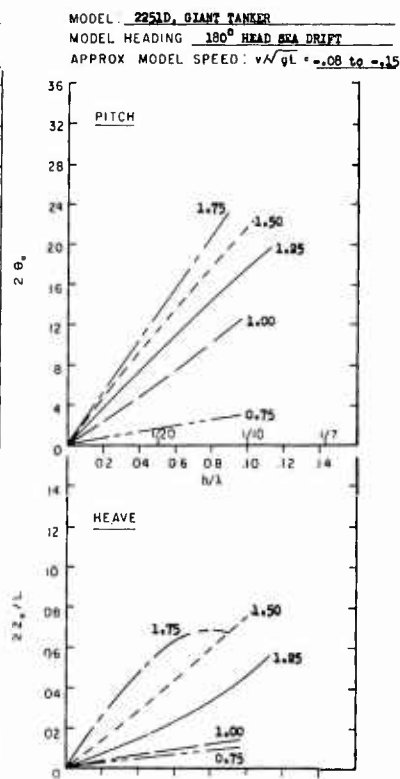


FIG. 24.

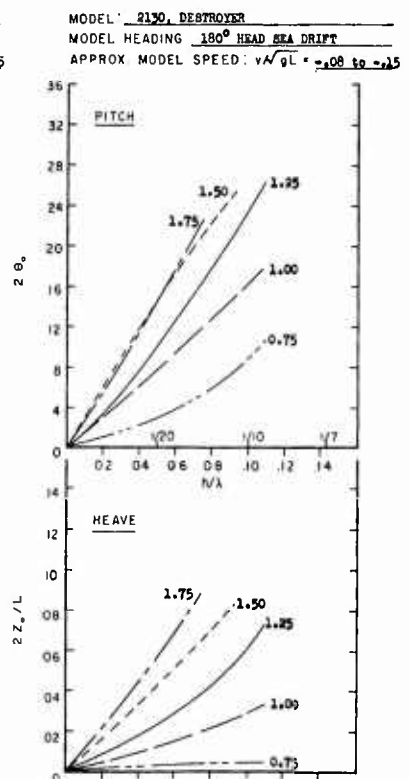


FIG. 25.

FIG. 20-25. TRENDS OF PITCH AND HEAVE AMPLITUDES WITH WAVE STEEPNESS.

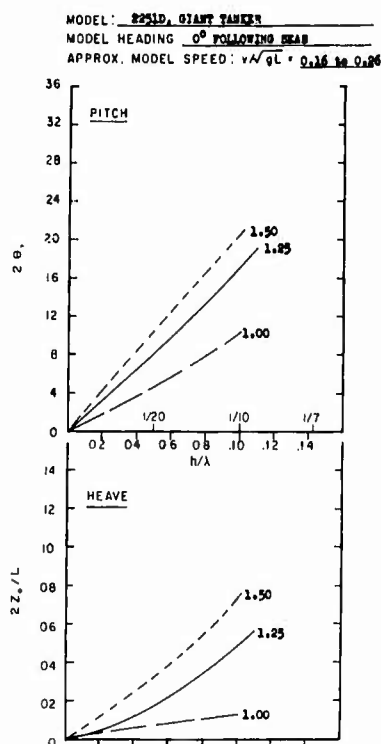


FIG. 26.

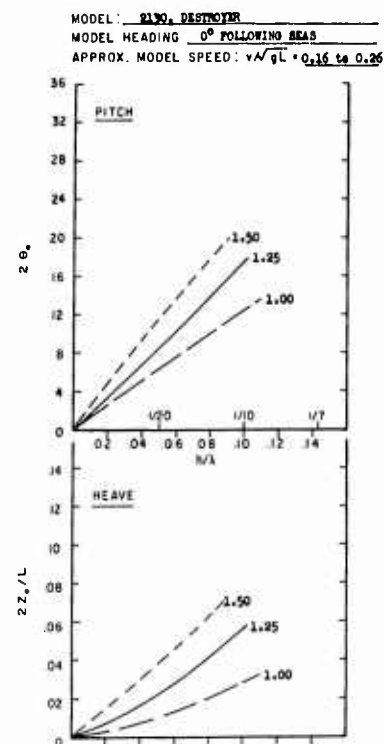


FIG. 27.

FIG. 26-27. TRENDS OF PITCH AND HEAVE AMPLITUDES WITH WAVE STEEPNESS.

$$\mu = C \cdot (h/\lambda) \cdot (\lambda/L)$$

$$\frac{d\mu}{d(h/\lambda)} = C \cdot (\lambda/L)$$

$$C = (L/\lambda) \cdot \frac{d\mu}{d(h/\lambda)}$$

Since the present data are summarized in terms of hog and sag, the sum of the slopes of the curves fitted through the test spots was multiplied by L/λ and used as the moderate wave bending moment range coefficient. Figure 32 shows a comparison of the bending moment range data measured in tests of destroyers. Unfortunately, in this instance the only test results available are of Model 2130 (from Ref. 4, 5) with the exception of one single point obtained by Sato in Japan in 1945 (Ref. 7). This point is shown in comparison with the results from the previous DL experiments and from the present experiment. Agreement is not considered to be too bad, considering the fact that in the present experiment no data were obtained at the low wave steepnesses. In Fig. 33 for the Giant Tanker the results from the present experiment are compared with those for three other models, Refs. 8, 9 and 10. All the models shown are similar in form and the agreement shown is considered good.

B. Classification of Trends

Even though the presentation of trends of bending moments and motions with wave steepness in Figs. 12-27 compresses the basic results five fold, it is still rather difficult to keep track of the differences in trend of bending moment and motions with wave steepness. Therefore an approximate numerical classification of the shape of the

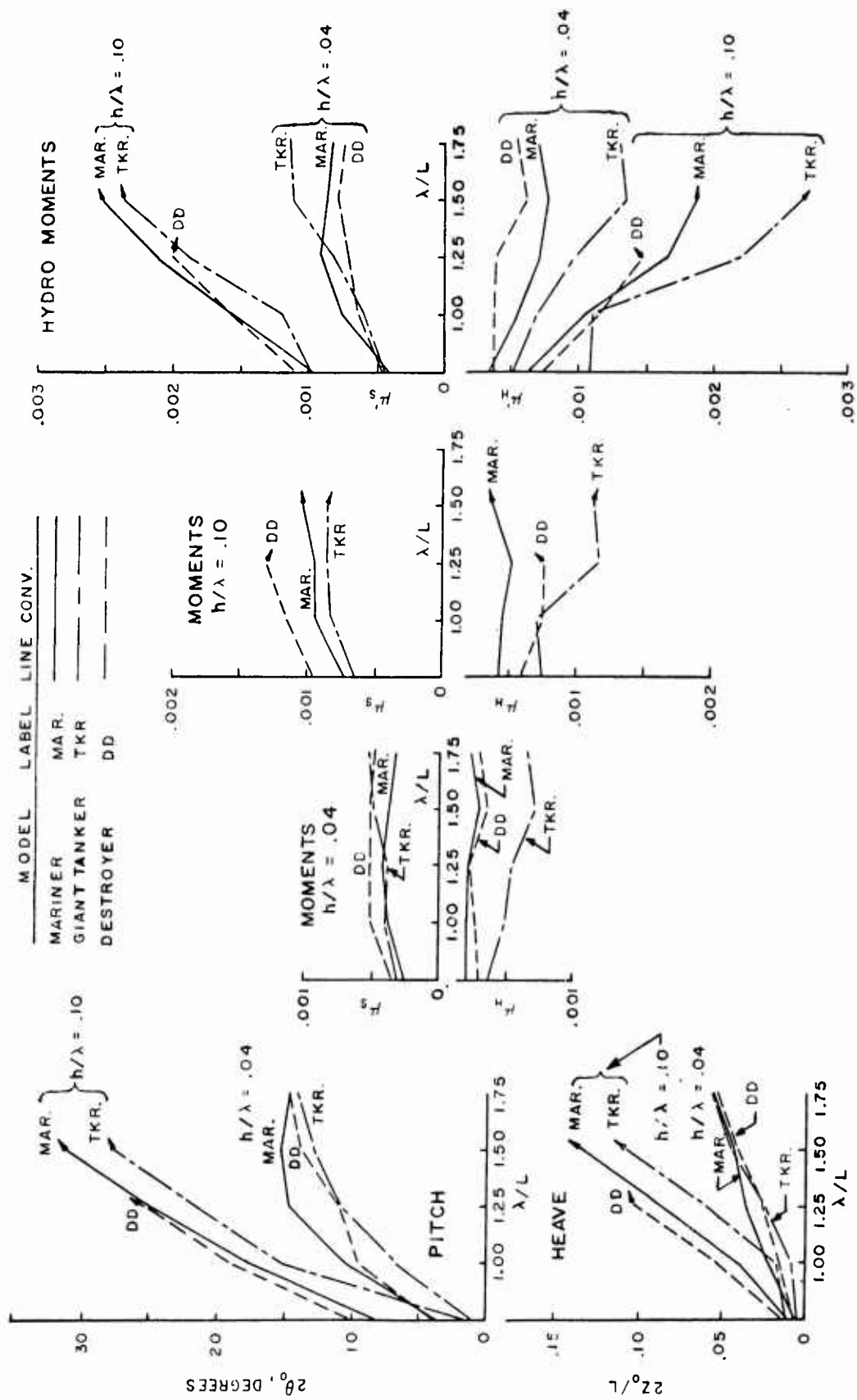


FIG. 28. CROSS PLOT OF FAIRED MOMENTS AND MOTIONS, HEAD SEAS, FR. NO. 0.12 TO 0.14.

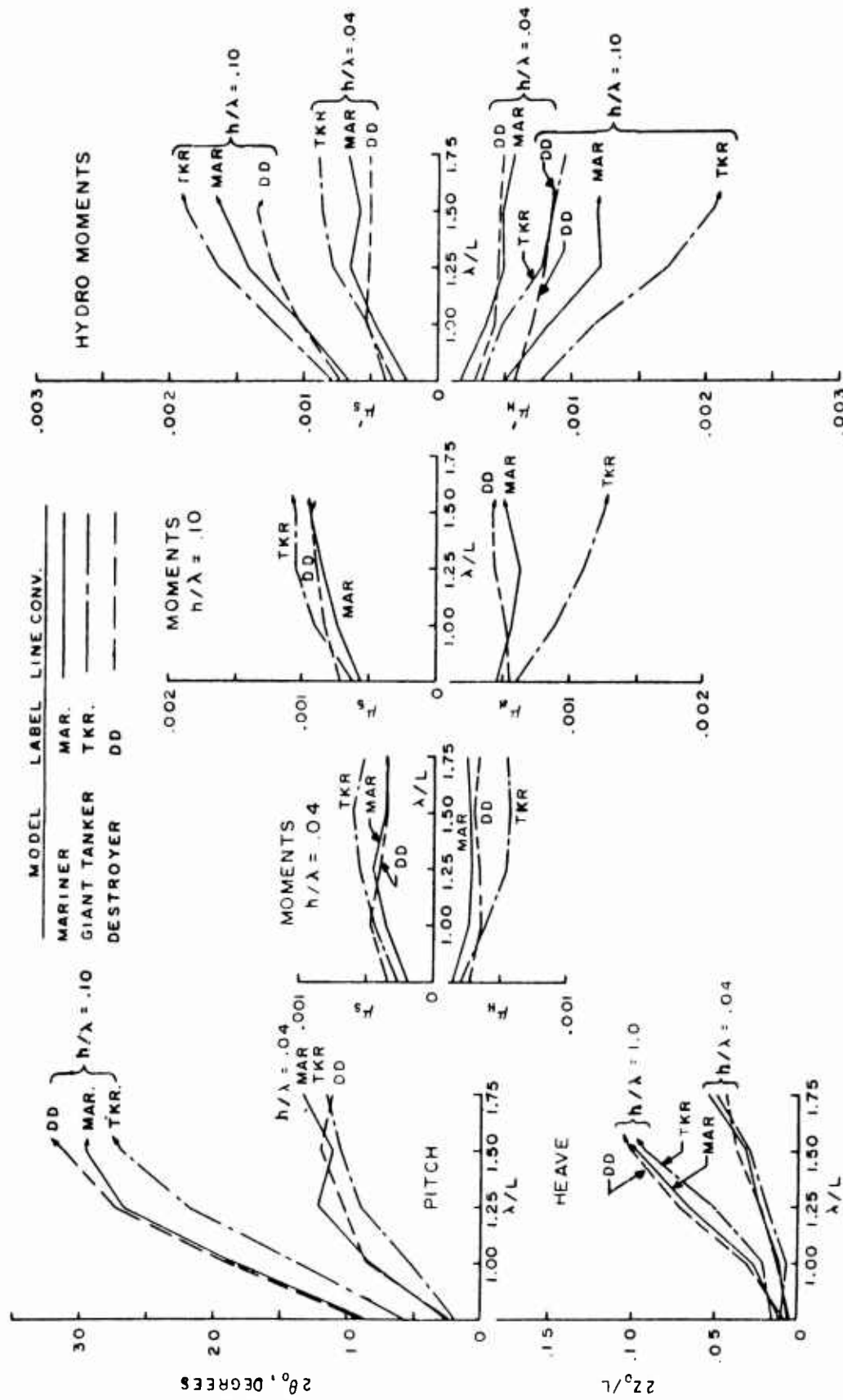


FIG. 29. CROSS PLOT OF FAIRED MOMENTS AND MOTIONS, HEAD SEAS, FR. NO. 0.0.0.

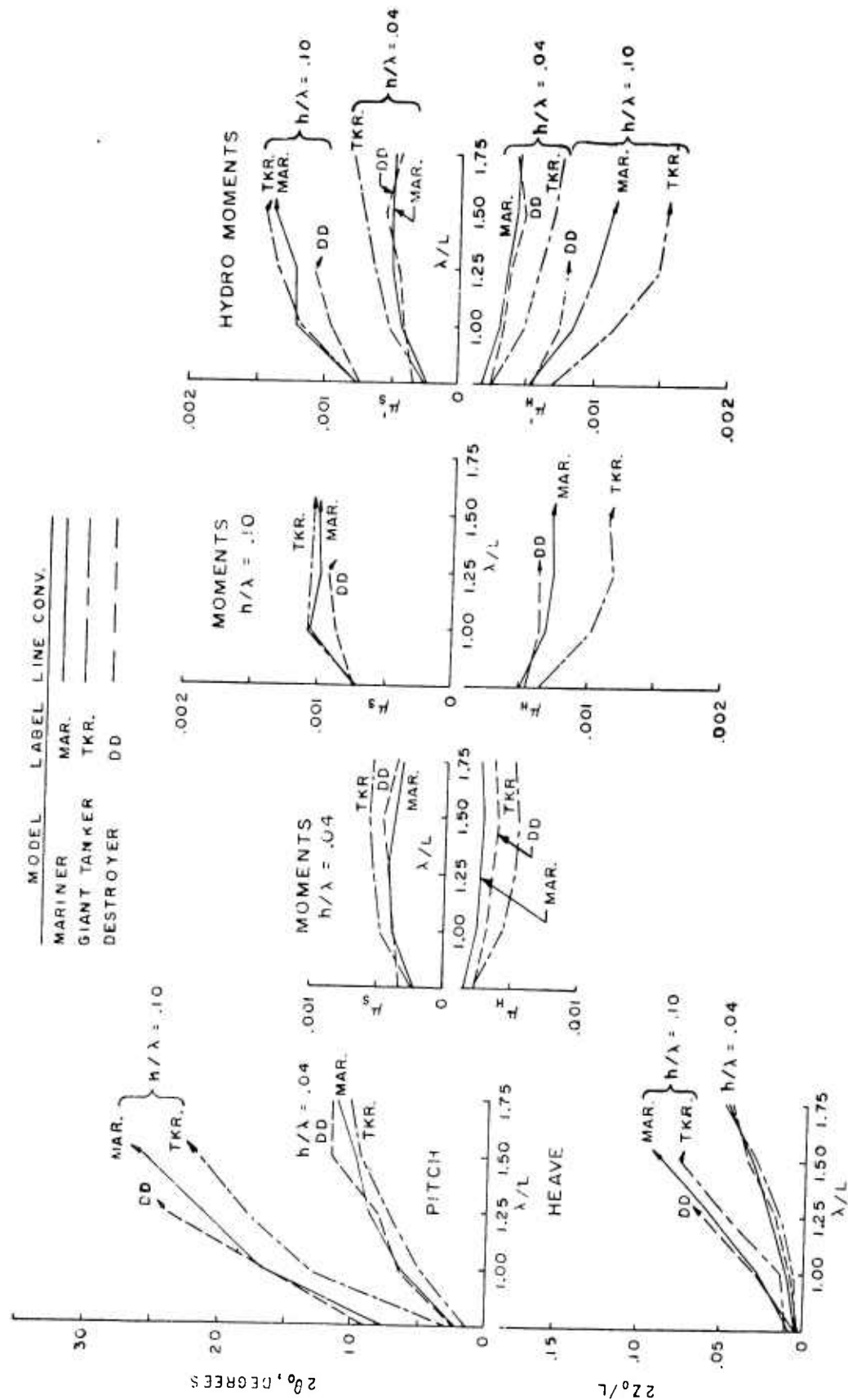


FIG. 30. CROSS PLOT OF FAIRED MOMENTS AND MOTIONS, HEAD SEAS, DRIFTING ASTERN, FR. NO. -0.08 to -0.15.

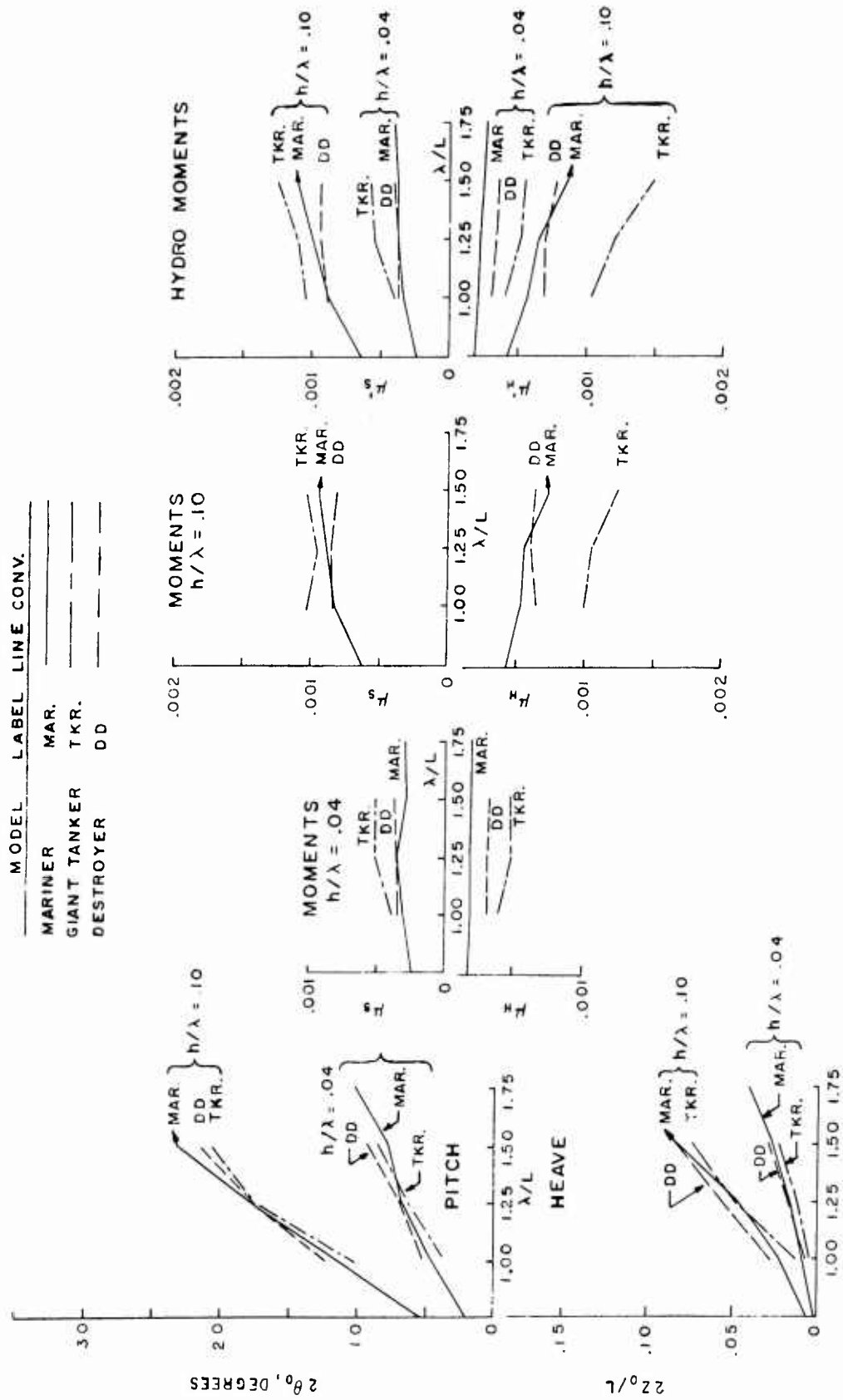
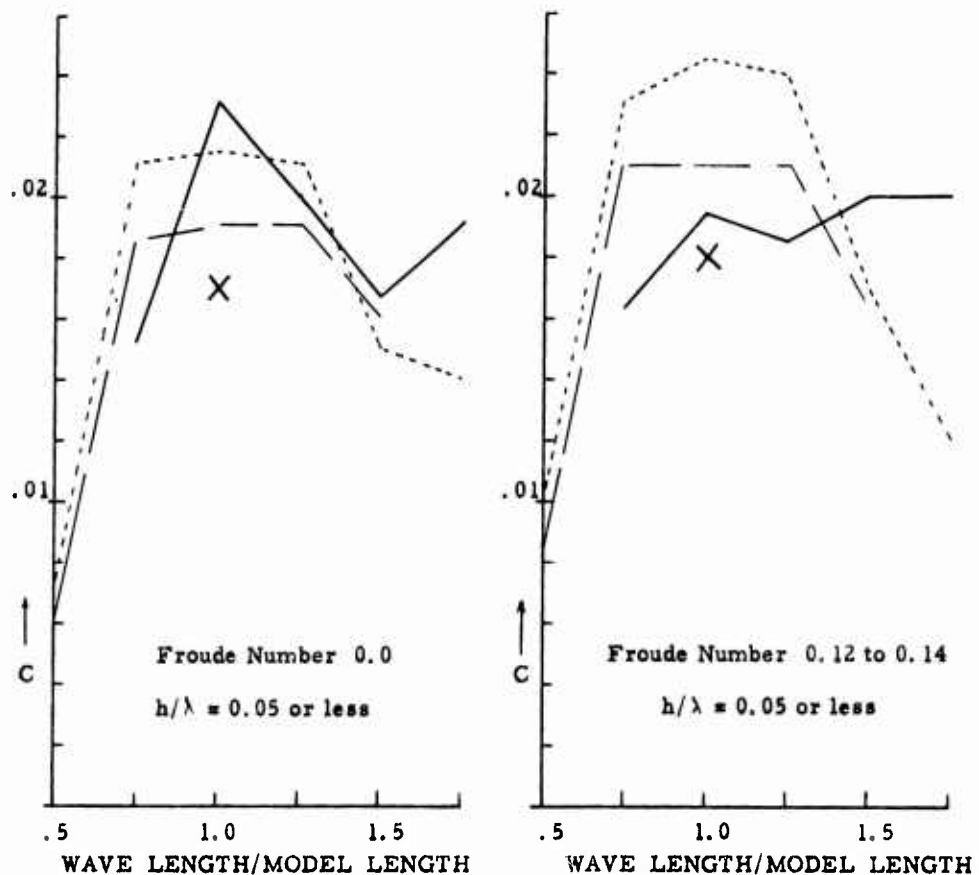


FIG. 31. CROSS PLOT OF FAIRED MOMENTS AND MOTIONS, FOLLOWING SEAS, FR. NO. 0.16 to 0.26.



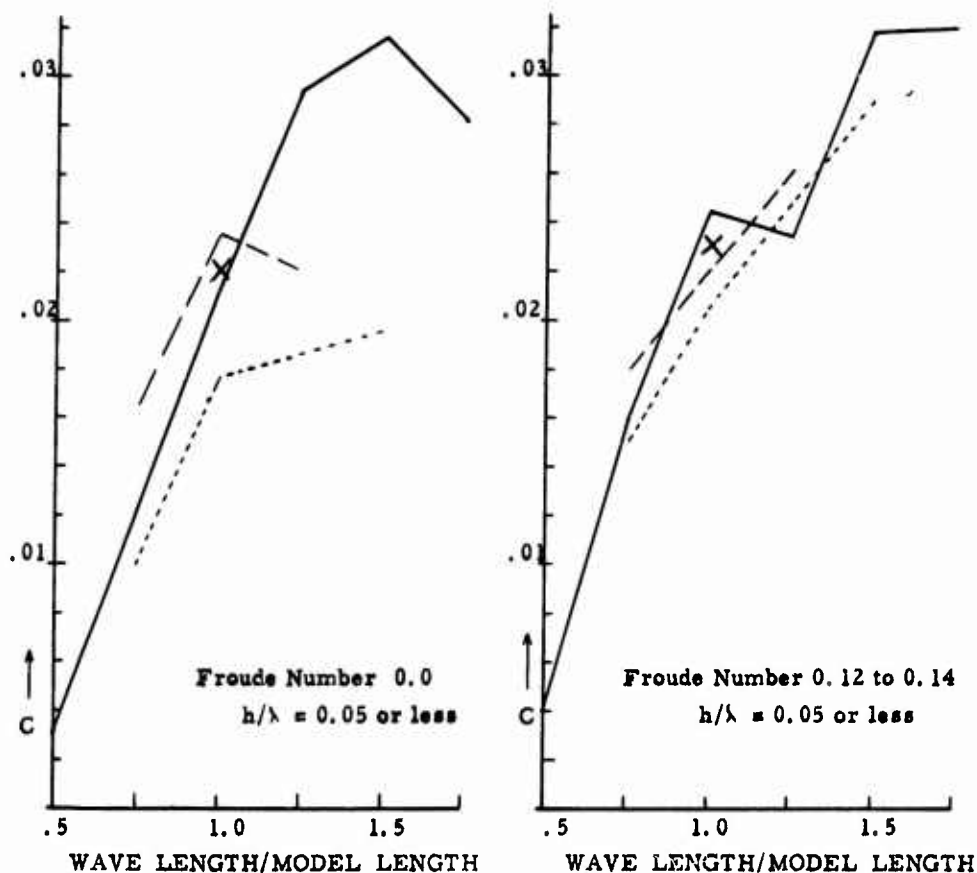
KEY AND SOURCE OF DATA

- Model 2130, $C_B = 0.55$
- X Destroyer, $C_B = 0.55$, "Model Experiments on the Longitudinal Strength of Ships Running Among Waves," Sato, M., SNA, Japan 1951.
- } Model 2130, Previous Davidson Laboratory Results, Report 656, 1958 and Report 810, 1962.

FIG. 32. COMPARISON OF BENDING MOMENT RANGES MEASURED IN THE DESTROYER WITH OTHER TEST RESULTS.

lines in Figs. 12-27 was made. Figure 34 summarizes the definition of the numerical criterion finally adopted and shows plotted examples.

The sketch at the right hand side of Fig. 34 illustrates the criterion, (γ) and the method of computation. In order to classify the shape of curve (B) in that sketch a straight line through the origin was first fitted to curve (B) over a region of wave steepness between 0.05 and 0.10. A least squares fitting technique was used. The difference between curve (B) and the fitted straight line (A) at a wave steepness of 0.10 was then evaluated (β). If this difference is negative (see Fig. 34) the curve B is convex upward, if the quantity β is positive, curve B is concave upwards. The straight line was fitted between wave steepnesses of 0.05 and 0.10 primarily because this is the region of wave steepness where actual data was obtained in all cases.



KEY AND SOURCE OF DATA

- Model 2251D, Tanker, $C_B = 0.80$
- - - - Series 60, $C_B = 0.80$, "Experimental Determination of Bending Moments for Three Models of Different Fullness in Regular Waves," DeDoes, J. C., Delft 1960.
- Tanker, $C_B = 0.78$, "Ship Model Bending Moments in Waves," Luzzi, P. C. and Kimball, E. D., M. I. T. 1957.
- × Series 57, $C_B = 0.80$, "Effect of Speed and Fullness on Hull Bending Moments in Waves," Dalzell, J., Davidson Lab. 1959

FIG. 33. COMPARISON OF BENDING MOMENT RANGES MEASURED IN THE TANKER WITH OTHER TEST RESULTS.

The quantity β is also almost directly proportional to the difference between the slope of curve (B) at a wave steepness of zero and the slope at a wave steepness of 0.10. This fact strengthens its use as a criterion.

It was felt that β should be normalized to account for variations in magnitude of the moments and motions, and it was therefore divided by the ordinate of the fitted curve (B) at a wave steepness of 0.10 (α , Fig. 34), to yield the numerical criterion, γ . For curves of the analytic form used for the computer fitting of the test data, γ is simply evaluated with the coefficients in the equation. The left hand side of Fig. 34 shows examples of curves with different γ criteria. The abscissa of this plot is wave steepness, the ordinate can be either bending moments or motions. Two

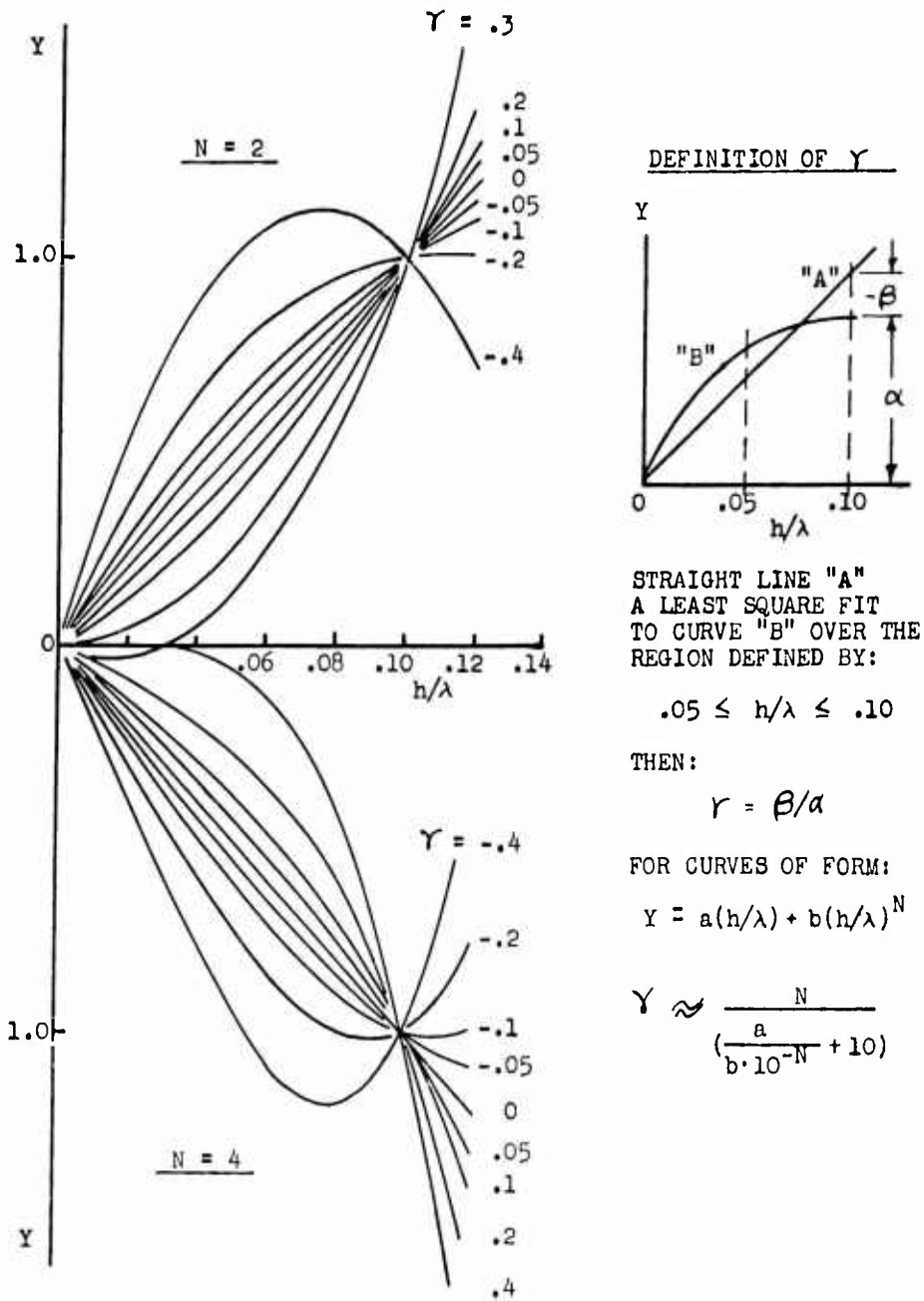


FIG. 34. NUMERICAL CLASSIFICATION OF FITTED CURVES: DEFINITION AND EXAMPLES.

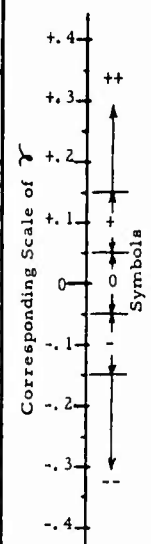
families of curves are plotted. The top family for an exponent of the second term in the equation equal to 2, the bottom family for an exponent of 4. The γ value for each curve is noted and it can be seen that the differences in shape between curves for $N = 4$ and $N = 2$ for the same value of γ are relatively small. It was seen that the percentage differences in ordinates between curves with γ values differing by 0.10 or less are something like the percentage scatter of data points shown in Ref. 6. It was therefore felt that it was pointless to present results from the numerical classification in fine numerical detail.

A value of γ was computed for each mean line shown in Figs. 12-27. The results were divided into five classes:

TABLE IV. CLASSIFICATION OF TRENDS WITH WAVE STEEPNESS OF MOMENT AND MOTIONS.

| Speed, Heading | λ/L | Sagging Moment | | | Hogging Moment | | | Pitch | | | Heave | | | Hydro. Sag | | | Hydro. Hog | | |
|----------------------|-------------|----------------|---------|-----------|----------------|---------|-----------|--------------|---------|-----------|--------------|---------|-----------|--------------|---------|-----------|--------------|---------|-----------|
| | | Giant Tanker | Mariner | Destroyer | Giant Tanker | Mariner | Destroyer | Giant Tanker | Mariner | Destroyer | Giant Tanker | Mariner | Destroyer | Giant Tanker | Mariner | Destroyer | Giant Tanker | Mariner | Destroyer |
| 0.12 to 0.14, 180° | 0.75 | - | + | 0 | - | - | - | 0 | - | 0 | 0 | - | 0 | 0 | 0 | 0 | 0 | 0 | 0 |
| | 1.00 | -* | 0* | 0* | -* | 0 | + | 0 | - | - | 0 | 0 | + | 0* | 0* | 0* | 0* | 0* | 0* |
| | 1.25 | -* | 0* | 0* | -* | 0 | + | 0 | - | - | 0 | 0 | + | 0* | 0* | 0* | 0* | 0* | 0* |
| | 1.50 | -* | 0* | 0* | -* | 0 | + | 0 | - | - | 0 | 0 | + | 0* | 0* | 0* | 0* | 0* | 0* |
| | 1.75 | -* | 0* | 0* | -* | 0 | + | 0 | - | - | 0 | 0 | + | 0* | 0* | 0* | 0* | 0* | 0* |
| 0.0, 180° | 0.75 | 0 | 0 | 0 | 0 | 0 | 0 | 0 | 0 | 0 | 0 | 0 | 0 | 0 | 0 | 0 | 0 | 0 | 0 |
| | 1.00 | - | - | - | 0 | - | - | 0 | - | 0 | 0 | 0 | 0 | 0 | 0 | 0 | 0 | 0 | 0 |
| | 1.25 | - | 0 | 0 | - | - | - | 0 | - | 0 | 0 | 0 | 0 | 0 | 0 | 0 | 0 | 0 | 0 |
| | 1.50 | - | 0 | 0 | - | - | - | 0 | 0 | 0 | 0 | 0 | 0 | 0 | 0 | 0 | 0 | 0 | 0 |
| | 1.75 | 0 | 0 | 0 | - | - | - | 0 | - | 0 | 0 | 0 | 0 | 0 | 0 | 0 | 0 | 0 | 0 |
| -0.08 to -0.15, 180° | 0.75 | 0 | + | - | 0 | 0 | 0 | 0 | + | + | 0 | - | 0 | + | - | 0 | 0 | 0 | 0 |
| | 1.00 | 0 | 0 | 0 | 0 | 0 | 0 | 0 | 0 | 0 | 0 | 0 | 0 | 0 | 0 | 0 | 0 | 0 | 0 |
| | 1.25 | - | 0 | 0 | 0 | 0 | 0 | 0 | 0 | 0 | 0 | 0 | 0 | 0 | 0 | 0 | 0 | 0 | 0 |
| | 1.50 | - | 0 | 0 | 0 | 0 | 0 | 0 | 0 | 0 | 0 | 0 | 0 | 0 | 0 | 0 | 0 | 0 | 0 |
| | 1.75 | - | 0 | 0 | 0 | 0 | 0 | 0 | 0 | 0 | 0 | 0 | 0 | 0 | 0 | 0 | 0 | 0 | 0 |
| 0.16 to 0.26, 0° | 1.00 | 0 | 0 | 0 | 0 | 0 | 0 | 0 | 0 | 0 | 0 | 0 | 0 | 0 | 0 | 0 | 0 | 0 | 0 |
| | 1.25 | - | 0 | 0 | 0 | 0 | 0 | 0 | 0 | 0 | 0 | 0 | 0 | 0 | 0 | 0 | 0 | 0 | 0 |
| | 1.50 | - | 0 | 0 | 0 | 0 | 0 | 0 | 0 | 0 | 0 | 0 | 0 | 0 | 0 | 0 | 0 | 0 | 0 |

NOTATION
*Trace Distorted by Impact
ND-No Data



- Class ++: Curves with γ greater than 0.15
- Class + : " " " between +.15 and +.05
- Class 0 : " " " +.05 and -.05
- Class - : " " " -.05 and -.15
- Class --: " " " less than -.15

If a curve falls in the third category one could almost call it a straight line. Curves in the second or fourth categories show the beginnings of a trend with wave steepness. If a curve falls in the first or fifth categories a definite trend is shown.

Results of the computations and classifications are summarized in Table IV, where results are shown separately for sagging moment, hogging moment, pitch amplitudes and heaving amplitudes as well as the approximate hydrodynamic sagging and hogging moments to be discussed subsequently. It may be noted that no computations were made for wave lengths of 0.5L in the head sea cases nor for 0.75L and 1.75L in the following sea case.

The corresponding results for the Parent Mariner model have been taken from Ref. 2 and are included in Table IV.

C. Maximum Bending Moments in Waves of Fixed Height

The cross plots of Fig. 28-31 are made on the basis of constant wave steepness. It was felt of interest to display the moments in extreme waves of constant height. The reason for this distinction was that the highest wave developed in the model tests is about 150 feet high to Giant Tanker scale. It is unclear whether such

an extreme wave does occur in deep water with any measurable frequency and it was felt that somewhat different conclusions might be drawn from cross plots of bending moments for constant wave height than are drawn from cross plots for constant wave steepness. Figures 35, 36 and 37 are cross plots of the faired bending moments of Figs. 12-19 for waves of a height equal to 10% of the ship length (full scale about 90 ft. for the tanker). An exception was made in the case of the 0.75L waves where the values for a wave steepness of 0.10 are shown. (This was done in order to avoid using points from an extrapolation of the curves fitted to the data.) Only the results for the three practical speed-heading conditions are shown. Results for both models are shown in each plot, as are the results for the Parent Mariner from Reference 2.

It was also felt of interest to display the approximate variation with speed of the maximum moment in waves 10% of the ship length in height. This has been done in Fig. 38 where the maximum moments shown in Figs. 35-37 are plotted according to speed. Points for the maximum moments in head seas at forward speed were evaluated directly from Figs. 12 and 13. Points are connected by straight lines in the head sea cases. The corresponding data for the Parent Mariner model from Ref. 2 is also shown.

D. Approximate Hydrodynamic Bending Moments

Since bending moments arise both as a result of the integration of water pressures and by virtue of acceleration of the mass of the model or ship, it was of interest in a first analysis to separate the hydrodynamic moment from the total measured moment. In so doing, various approximations were made in order to allow an approximate treatment of the mass of data obtained in this project rather than detailed study of fewer cases. The derivation of the moment due to accelerations of the model is shown in the Appendix. In general, the moments due to the acceleration of model mass in the forebody are unequal to the moments produced by acceleration of the model mass in the aft body. Therefore the average of the moments in the forebody and afterbody due to acceleration of mass was computed. The final approximation to the average moment due to acceleration is as follows:

$$\begin{aligned} \bar{M}_{FA} = & \left[A_2 \omega_e^2 (2Z_o/L) \cos \delta + C_2 \omega_e^2 (2\theta_o) \cos \epsilon \right] \cos \omega_e t \\ & + \left[A_2 \omega_e^2 (2Z_o/L) \sin \delta + C_2 \omega_e^2 (2\theta_o) \sin \epsilon \right] \sin \omega_e t \end{aligned}$$

(Appendix Equation 14)

where:

$(2Z_o/L)$ = heaving double amplitude, non-dimensional

$(2\theta_o)$ = pitching double amplitude, degrees

δ, ϵ = phase lags of motions following bending moment

ω_e = wave encounter frequency

t = time

A_2, C_2 = coefficients

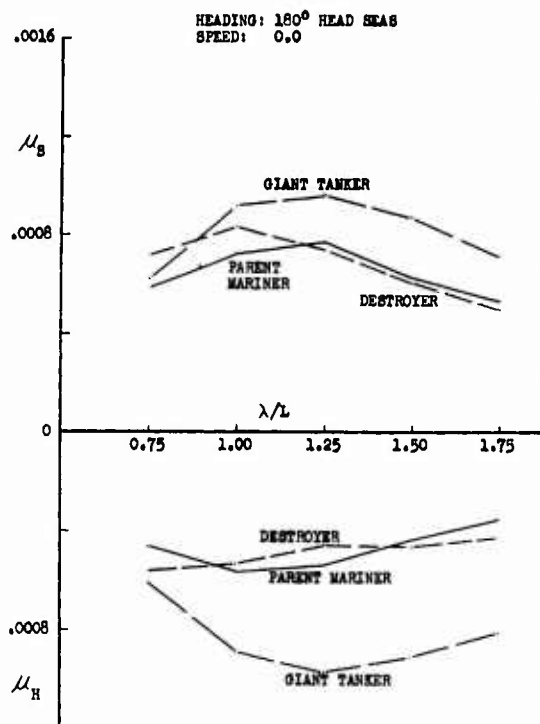


FIG. 35.

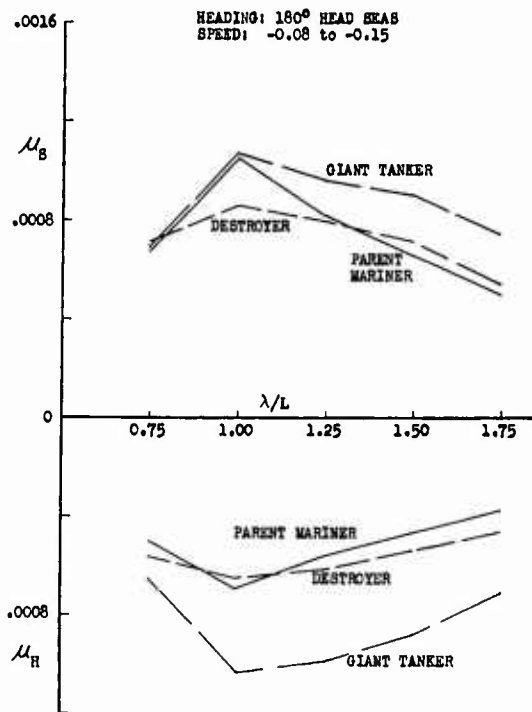


FIG. 36.

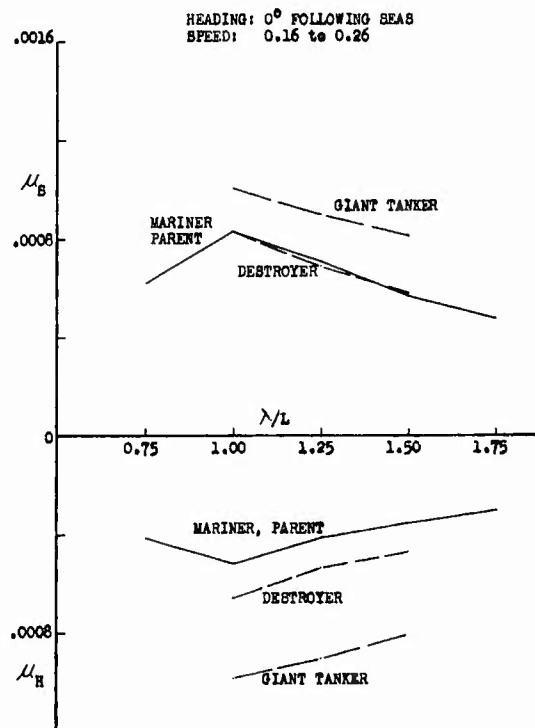


FIG. 37.

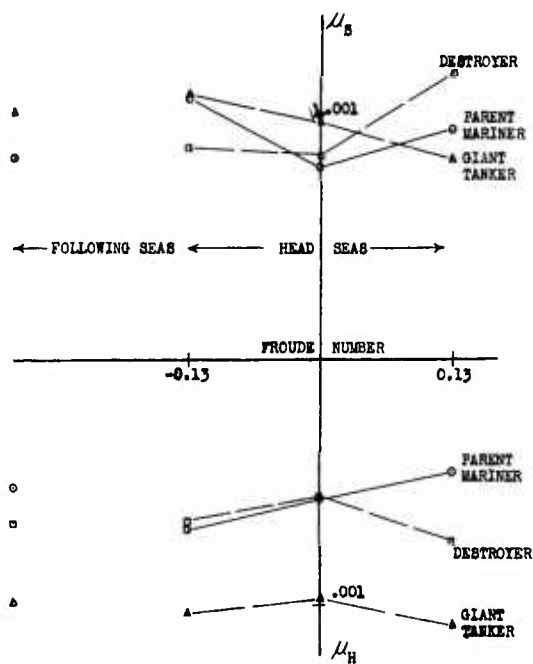


FIG. 38. VARIATIONS WITH SPEED AND HEADING OF MAXIMUM MOMENT IN $L/10$ WAVES OF ANY LENGTH.

FIG. 35-37. CROSS PLOTS OF FAIRED BENDING MOMENTS IN $L/10$ WAVES OF VARIOUS LENGTHS.

The coefficients A_2 and C_2 involve only physical parameters of the models. A_2 is proportional to the average of the mass moments about amidships forward and aft. C_2 involves the difference of the mass moments of inertia about amidships forward and aft, and a product of model LCG with LCG's of forebody and afterbody (see Appendix). M_{FA} was divided by the quantity $(\rho g L^3 B)$ to non-dimensionalize. It was then evaluated for all the model, speed, heading and wave length combinations in the test program except for those involving the zero speed following sea condition or the 0.50L wave length. The faired mean lines through the motions test data were used and results were calculated for values of wave steepness from 0.02 to 0.12 in steps of 0.02.

Since the expression is a harmonic function with a phase lag relative to the maximum sagging moment, the four terms of this equation were evaluated separately. An inspection of the results showed, (1) that the sum of the two first terms (those multiplying cosine (ωt)) was always negative, (2) that the sum of the last two terms (multiplying sine (ωt)) was usually small relative to the sum of the first two terms, (3) that the second term of the equation (involving pitching amplitude) was normally small relative to the first term. In order to derive an approximate hydrodynamic bending moment, it was necessary to subtract the average bending moment due to acceleration from the measured moments. In order to do this with the data at hand and without going back to the original test record, it was necessary to assume that the bending moment was co-sinusoidal. A vector subtraction of the foregoing expression was partially performed under the above assumption. It was found that the differences between a vector subtraction and a subtraction of the sum of the first two terms from the sagging and hogging moment amplitudes were less than 5% of the total in all but about 10% of all the cases computed. (In this last 10% of the computations the differences were at worst 10%). Thus, instead of assuming co-sinusoidal bending moments and doing a vector subtraction, an approximate hydrodynamic sagging and hogging moment was obtained by subtracting the sum of the first two terms of the above equation from the measured sagging and hogging amplitudes. Since the sum of the first two terms of \bar{M}_{FA} is always negative the hydrodynamic moment is always larger than the measured moment. Because of the definition of the phases δ , and ϵ , this process is similar to subtracting the moments due to acceleration computed at the time of maximum sag or hogging moment from the measured sagging or hogging moment. The expression for the approximate hydrodynamic sagging and hogging moments is shown below:

$$\mu_S'' = \mu_S - \bar{M}_{RE} / \rho g L^3 B$$

$$\mu_H'' = \mu_H - \bar{M}_{RE} / \rho g L^3 B$$

where:

$$\bar{M}_{RE} = A_2 \omega_e^2 (2Z_o/L) \cos \delta + C_2 \omega_e^2 (2\theta_o) \cos \epsilon$$

Figures 39 and 40 show examples of the approximate hydrodynamic bending moment plotted to a base of wave steepness.

It is proper to compare Fig. 39 with Fig. 14, and while the scales are slightly different, the impression was obtained that the hydrodynamic moments show a smaller departure from a straight line trend with wave steepness than do the measured moments. Somewhat the same conclusion was drawn from a comparison of Fig. 40 with Fig. 15. Since the curves of "Hydrodynamic" moments appeared reasonably well behaved, a numerical approximation to the trend classification criterion (γ) was devised and this computation was done for all of the resulting curves of hydrodynamic bending moments versus wave steepness. The results were classified as were the results from the calculation for the measured moments and are summarized in Table IV under the heading Hydro Sag,

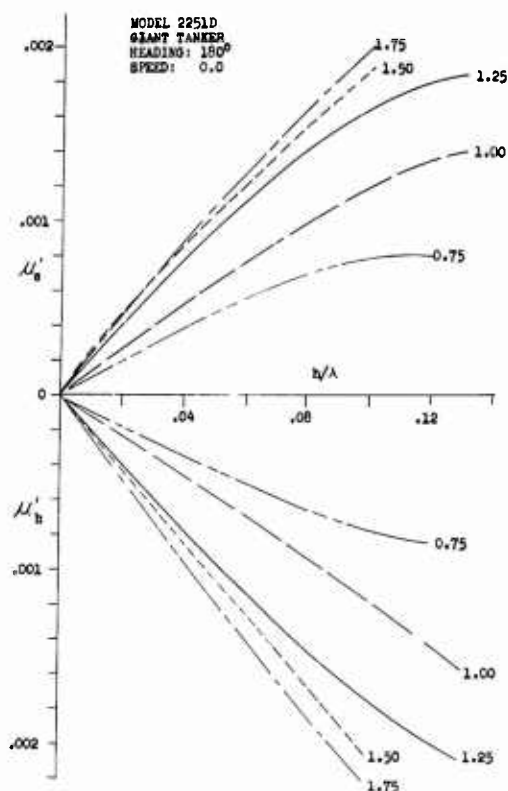


FIG. 39.

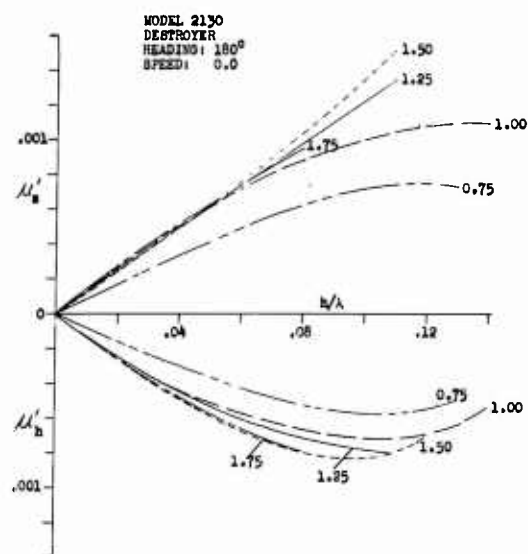


FIG. 40.

FIG. 39-40. APPROXIMATE HYDRODYNAMIC BENDING MOMENTS.

and Hydro Hog. Cross plots of these hydrodynamic moments were made for wave steepnesses of 0.04 and 0.10 and are included in Figs. 28-31 at the far right of each figure.

DISCUSSION

A. Trends of Bending Moment with Wave Steepness

1. Detailed Discussion of Figures 12 to 19.

It is thought to be important to keep in mind the fact that the smooth curves plotted in Figs. 12 to 27 do not represent the variation of one smooth, easily measurable experimental quantity with another. They represent the end product in a data reduction process in which about 10,000 numerical measurements from approximately 200 oscillograph records were compressed into 8 charts. Each line plotted is a least squares fit of an equation to a number of test spots. Each test spot is the average of 5 to 20 maximum sagging (or hogging) moments measured from a time history and plotted against an average wave steepness also measured from a time history.

Reference 6 contains references to probable distortion of the time histories of bending moment by relatively long duration impacts, and it was worthwhile to examine, at the source, the faired lines plotted in Figs. 12-19 with respect to how reasonable a fit to the test spots was attained in each case and to note under what circumstances the above mentioned quasi-impacts were recorded. The results of such an examination follows:

a) Figures 12 and 13, Head Seas, Forward Speed

In Fig. 12 for the Giant Tanker it can be seen that the trends of bending moment with wave steepness generally indicate that some limiting value may exist at very high wave steepnesses. Some distortion of both hogging and sagging results for the 1.0, 1.25 and 1.50L waves is thought to have occurred due to quasi-impacts. The fit of the faired lines to the test spots is reasonably good in all cases except for the hogging moment in 1.50L waves where an over-fit may have occurred.

In Fig. 13 for the Destroyer a different picture of trends of moment with wave steepness is seen. The faired lines tend to be straighter than those for the Giant Tanker. The fit of the faired lines to the test points is good in all cases except for the hogging moments in 1.0 and 1.25L waves. Omission of the one or two points in question on each curve would not change the trends of the curves. Sagging traces were apparently influenced by quasi-impacts in all of the waves from 1.0 to 1.50L. In addition in the 1.0L and 1.25L waves, suspicion exists that the hogging moments were influenced by green water hitting the superstructure of the model. This may account for the scatter of the hogging moment data in these two wave lengths.

b) Figures 14 and 15, Head Seas, Zero Speed

In Fig. 14 for the Giant Tanker, the fit of the faired lines to the test spots is good in all cases and no quasi-impacts were noted. The general appearance of the curves is similar to that of Fig. 12. It may be noted from these plots that the wave hogging moment is appreciably larger than the wave sagging moment. This is a departure from the trends of moments of all other models tested, including those of Ref. 2.

The general appearance of Fig. 15 for the Destroyer at zero speed is much different than that of Fig. 13 (Destroyer at forward speed). This difference may be due to the absence of quasi-impacts in the zero speed case. The fit of the faired lines to the test spots is reasonably good in all cases.

c) Figures 16 and 17, Head Seas, Drifting Astern

The plotted curves in both Fig. 16 and 17 are straighter than in the previous head sea cases. The fit of the faired lines to the data points is good in all cases and no quasi-impact was noted.

d) Figures 18 and 19, Following Seas, Forward Speed

These two figures again show a relatively straight trend of moments with wave steepness. No quasi-impacts were noted. The fit of the lines to the test spots is reasonable, considering the fact that all lines were fitted to test spots, each of which was derived from quite small numbers of recorded encounter cycles.

B. Trends of Motions Amplitudes with Wave Steepness

In the plots for trends of motion amplitudes with wave steepness (Figs. 20 through 27) all of the faired lines fit the test spots reasonably well with two exceptions. The first exception is noted in Fig. 24 for the Giant Tanker in head seas, drifting astern. In this figure the trend of heaving amplitude with wave steepness in the 1.75L wave differs from the trends of the other wave lengths and an examination of the original data disclosed a poor fit to the test spots. If one of two points which were fitted poorly were omitted, the trend would change to one similar to that of the 1.5L wave, omission of the other point would not alter the trend. There is no known reason to discard either point. The other exception is noted in Fig. 21 for the

Destroyer in head seas at high speed. Considerable scatter of pitching amplitude test spots about the faired lines was seen in the 1.25L wave results. A general view of the trends of motion amplitudes with wave steepness for these two models discloses no radical differences in types of trends as far as motions are concerned.

C. Results of Numerical Classification of Trends with Wave Steepness

Table IV summarizes the results of the classification of trends of bending moments with wave steepness. Classification results applicable to the Mariner were taken from Ref. 2 and are shown between those for the Tanker and Destroyer. It is noted that zero in the table signifies a relatively straight line variation. The minus sign denotes the beginning of a convex upward trend, two minus signs denote a definite convex upward trend. Insofar as ascertaining maximum physically possible moments is concerned, the minus-minus designation is the most favorable situation. On the other hand, a plus-plus designation means that the moments or motions are concave upward and this is a distinctly bad indication of an upper bound. The asterisks indicate those cases where it was noted that a suspicion of distortion of moment trace by impact was present. The results in the table for the 1.75L waves were in almost all cases obtained by extrapolating the mean lines somewhat further than was done in Figs. 12 through 27. This means that there was not enough initial data present in the higher wave steepnesses to justify extending the line to this extent and the classification of trend results must be viewed in this light. The same is true for the 1.50L case for the Destroyer model in head seas at forward speed and drifting astern.

The first six columns of Table IV are the most important to the main objective of this investigation; that is, to confirm the existence of an upper bound on bending moments.

The following table summarizes the incidence of the various classification results for sag and hog:

| Class | Incidence, % of Total | |
|-------|-----------------------|-----|
| | Sag | Hog |
| ++ | 0 | 0 |
| + | 8 | 11 |
| 0 | 55 | 35 |
| - | 28 | 30 |
| -- | 9 | 24 |

No double plus entry occurs in the first six columns of Table IV and thus the only convex upward trend of bending moments with wave steepness which is likely to be encountered is a weak divergence from a straight line.

On the positive side of the question of the existence of an upper bound is the incidence of double negative signs in Table IV -- 18 cases in all. Half of these occur in the head sea, forward speed case. So far as the extreme waves are concerned Ref. 2 concludes that this case is impractical for the Mariner. Since the tanker-type ship is designed for lower Froude numbers than the Mariner it will be even less well equipped to negotiate waves from 1/15 to 1/9 steepness. Of the three ship types, the Destroyer has the most chance of being able to negotiate some waves of greater than 1/15 steepness by virtue of its greater installed specific power. There is a serious question, however, of how long the Destroyer type could survive with the enormous quantities of green water impacting against the superstructure characteristic of high forward speed in the waves at the high end of the steepness range.

It is felt, as in Ref. 2, that the head sea, forward speed case presented represents an impractical situation for the commercial ship types and an improbable

case for the Destroyer. In view of the fact that the bending moments at lower speeds are not radically lower than those at the forward speed, especially in wave steepnesses less than about $1/15$, the nine cases of strong limiting trends at the forward speed shown in Table IV become of secondary importance.

Excluding the head sea, forward speed case, seven of the nine cases where a decided limiting trend is shown in Table IV apply to the Destroyer model. It would appear that a definite wave hogging moment limit has been approached for the Destroyer, within the experimental range of wave steepnesses, for model speeds in head seas between zero and drifting astern. The entries in the sagging moment column for the Destroyer on the other hand, indicate that no definite limit was found within the experimental range of wave steepnesses, although one may exist at higher wave steepnesses.

The absolute moment scales in Figs. 15 and 17 for the Destroyer show that the design moment based on the implied hogging limit would be about equal to the $L/20$ standard hogging calculation moment. Whether or not such a design limit would be useful in this particular case is open to question since it is about equal to the magnitude (on the absolute scale) of the highest sagging moments measured.

Again excluding the head sea forward speed case, the table shows that the hogging moments for the Giant Tanker have less tendency to level out than those for the Mariner of Ref. 2, and that the reverse tends to be true for the sagging moments.

Considering the two commercial forms, most of the entries in the table are zeros which indicate a more or less straight line variation of bending moment with wave steepness. Single minus signs which indicate the beginning of a leveling out trend are the next most frequent symbols. In the case of the single minus sign, the limiting moment would occur at a wave steepness exceeding $1/9$. It is clear that in order to attain consistent and definite limits on bending moments for both commercial forms, wave steepnesses up to the theoretical deep water maximum must be considered and that it is possible that entry into the region of standing waves where greater steepnesses are possible would be required. It is possible that this course of action would be as far away from practicability as the high forward speed case in head seas, since the present range of data ended with wave heights which, scaled to suit a 500 foot ship, were about equivalent to the highest waves reliably reported to have occurred at sea.

A comparison of the results of the classification of trends for the hydrodynamic sagging and hogging moments with those for the measured sagging and hogging moments shows much the same results as was shown in a similar comparison in Ref. 2. If the measured sagging and hogging moments are converted to approximate hydrodynamic sagging and hogging moments using the measured pitch and heave amplitudes, a general straightening of the trends with wave steepness is seen. This implies that any limiting trends in measured sagging and hogging moments are as closely related to the motions and the weight distribution of the model as to net non-linearities in hydrodynamic pressure on the model.

D. Additional Confirmation of the Results of Section C.

The practical basis of the conclusions of Section C hinges on the trend of the moments measured in the most severe wave lengths. Limiting trends displayed in other wave lengths may have little practical significance. In order to help confirm the conclusions obtained, a fresh start on the analysis was made without benefit of fitted lines or numerical manipulation. Reference 6 was consulted and every test point obtained in any wave condition and at all of the four test speeds was plotted on a single chart for each model. The only differentiation between points which was made was between those for the impractical head sea-forward speed case (solid circles) and those for all other speeds (open circles).

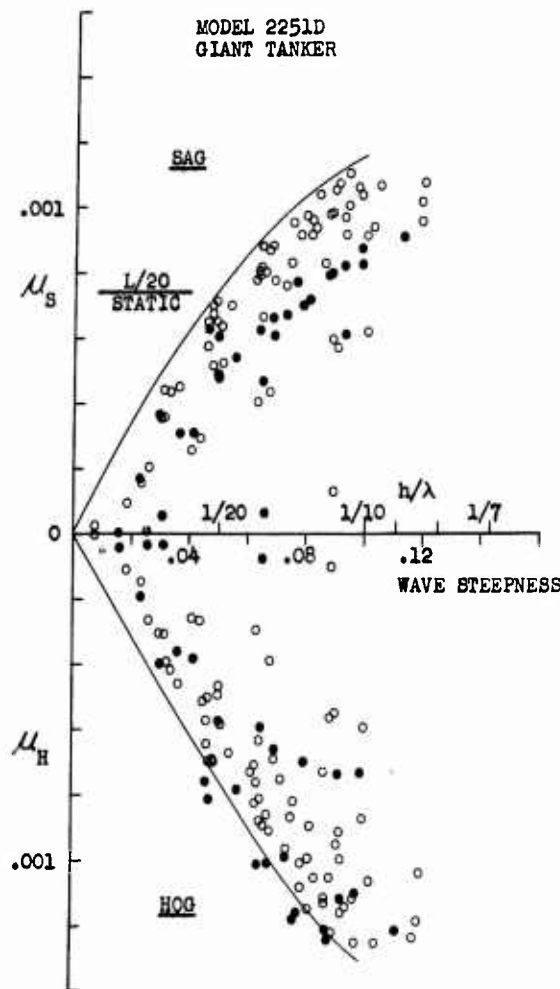


FIG. 41.

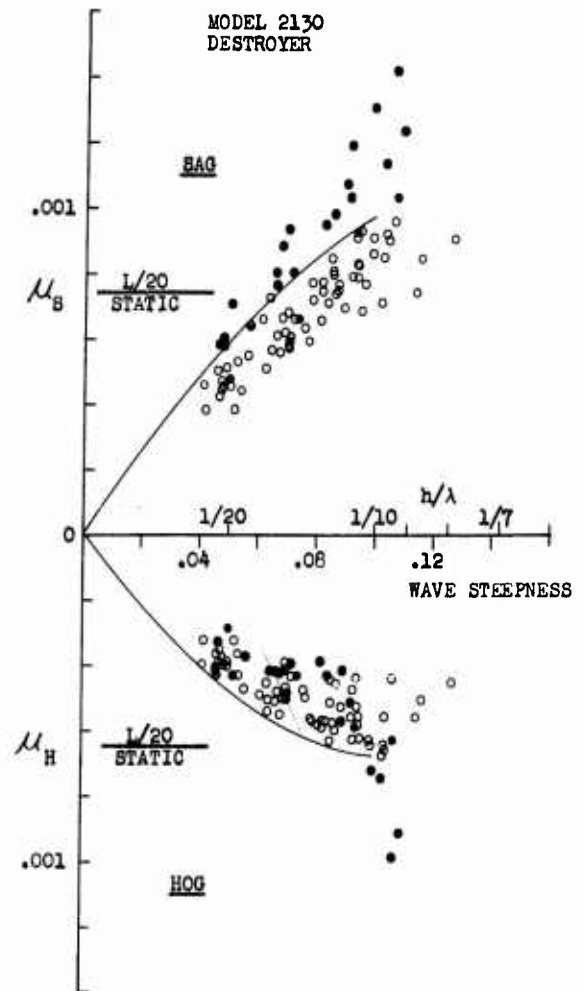


FIG. 42.

FIG. 41-42. MEASURED BENDING MOMENT DATA, ALL WAVE LENGTHS AND SPEEDS.

The results are shown in Figs. 41 and 42. Envelopes to the scatter of points were drawn up to a wave steepness of 0.10, excluding the points for the head sea-forward speed case. The envelopes were terminated at $h/\lambda = 0.10$ because the long wave lengths which contribute many of the highest moments are not well represented beyond this point. It can be seen that the envelopes drawn for the Giant Tanker (Fig. 41) imply no limit on moments in wave steepnesses less than $1/9$, a result similar to that for the Mariner in Ref. 2. If the head seas-forward speed case be disregarded in Fig. 42, the envelope shown for the Destroyer sagging moments also implies no limit on moments at a wave steepness less than $1/9$. The envelope for hogging moments on the same figure does indicate a limit reached at a wave steepness of about $1/9$, in agreement with the results of Section C. If the head sea, forward speed case be counted, this limit does not apply.

It is interesting to compare these results with those of Ref. 11. The experimental work of Ref. 11 was quite different than that reported herein in that it dealt with irregular model seas. It was similar in that the model utilized was the same destroyer model used herein, and in that the severity of the irregular waves was comparable to the severity of the regular waves of this study. Like the present results,

those of Ref. 11 imply that midship bending moment ranges are proportional to wave steepness over a very large range of wave steepnesses. (No distinction could be made in Ref. 11 between hogging and sagging moment trends.) The results of Ref. 11 also imply that midship bending moments have a mild limiting trend with wave steepness as wave severity is increased beyond that corresponding to State 6. It is therefore considered likely that the trends shown herein approximate those expected for significant bending moment amplitudes in random seas of increasing severity.

E. Bending Moments in Extreme Waves of Constant Height

Figures 35, 36 and 37 are cross plots of bending moments for the three practical speed cases where the wave heights are fixed at 10% of the model length. As in Ref. 2, it can be seen that the maximum moments in waves of fixed height tend to occur in the 1.0 and 1.25L wave lengths. If a design wave height can be established this is an alternate approach to an upper limit on bending moments, but is not a physical limit. Figure 38 shows the maxima of the bending moments in waves 10% of the model length high plotted on a base of speed. It can be seen that these maximum wave moments do not vary radically with speed and thus the finding of Ref. 2 which says, in effect, that no radical alteration in the magnitude of extreme bending moments can be made by changes in speed apparently hold true also for the Giant Tanker and the Destroyer.

F. Comparison Between Models

With the exception of the sagging moments in the head seas, forward speed case, where quasi-impacts were suspected, bending moments of the three models tended to increase substantially in order of increasing fullness. (Figures 28-31.) This progression was largely unaltered when the differing weight distributions and motions were used to derive approximate hydrodynamic moments. Conspicuous were the large wave hogging moments observed for the Giant Tanker model. In most cases motions amplitudes varied between the models only as much as the observed variation between the variants of the Mariner model shown in Ref. 2. Since the hydrodynamic moments of Ref. 2 did not show wide differences between models, it is supposed that the motions amplitudes themselves were not the major factor in the differences between model bending moments shown in Figs. 28-31. In effect, the non-dimensionalizing process utilized in this report results in bending moments for models of different lengths being reduced to moments for a constant ship length. Within this "length," displacement and form can vary widely without affecting the non-dimensionalizing factor ($1/\rho g L^3 B$). It is therefore not surprising that differences between hydrodynamic moments of the three models occur in the presentation of Figs. 28-31.

CONCLUSIONS

1. It appears on the basis of these studies and those of Ref. 2 that design wave bending moments are essentially proportional to wave heights which actually may be encountered.
2. The present studies, by establishing more firmly the grossly linear dependence of moments on wave heights over a considerable range of wave severity, has strengthened the case for determining design moments on the basis of statistical analysis of sea waves and/or the resulting moments.

3. This investigation and that of Ref. 2 included two end points of the spectrum of commercial cargo carrying ship types and it is concluded that for commercial type ships, within the practical operational limits in extreme head or following seas, no significant limit of midship wave bending moments is to be expected as wave steepness is increased up to a value of about $1/9$.
4. The above conclusion also applies to the sagging moments observed in the typical naval ship type tested but not for the wave hogging moments. Indications were found that an upper limit of hogging moments exists for this type, in extreme head seas, at a wave steepness in the vicinity of $1/9$.

RECOMMENDATIONS

The present study involved itself only with midship bending moments for reasons of economy, even though it was known that under certain conditions higher wave bending moments may develop elsewhere along the ship length. It is considered of importance to ascertain if the conclusions of this study also hold for moments all along the length of the ship. If similar conclusions can be drawn for moments elsewhere along the length of the ship no further development of the present experiments would be recommended, at least for commercial ship types.

ACKNOWLEDGEMENTS

The author wishes to acknowledge with thanks the excellent guidance and stimulus extended by the Project Advisory Committee headed by Mr. M. Forrest. The assistance rendered by a large number of members of the Davidson Laboratory staff is also acknowledged with thanks. Prominent among the many contributors were Messrs. E. Numata, S. Chuang, Y. Chey, R. Clapp and W. Klosinski of the Ship Research Division; Miss A. VonZumbusch and Mr. F. Behrens of the Computing Department, Mr. H. Deroian of the Photo Department, and Mrs. M. Brovarone, Secretary.

Much of the data reduction was done on the IBM 1620 Computer now being operated as part of the Computer Center of the Stevens Institute of Technology, which is partly supported by the National Science Foundation.

REFERENCES

1. Lewis, E.V. and Gerard, G.: "A Long Range Research Program in Ship Structural Design," Ship Structure Committee, Serial SSC-124, November 1959.
2. Dalzell, J.F.: "An Investigation of Midship Bending Moments Experienced in Extreme Regular Waves by Models of the Mariner Type Ship and Three Variants." OTS Report PB 181508.
3. Nichols, W.O. Rubin, M.L. and Danielson, R.V.: "Some Aspects of Large Tanker Design," SNAME Transactions, Vol. 68, 1960.
4. Lewis, E.V. and Dalzell, J.F.: "Motion, Bending Moment and Shear Measurements on a Destroyer Model in Waves," ETT Report 656, April 1958.
5. Dalzell, J.F.: "Cross Spectral Analysis of Ship Model Motions: A Destroyer Model in Irregular Long Crested Head Seas," DL Report 810, April 1962.

6. Dalzell, J.F.: "An Investigation of Midship Bending Moments Experienced in Extreme Regular Waves by Models of a Tanker and a Destroyer," DL Report 927, November 1962.
7. Sato, M.: "Model Experiments on the Longitudinal Strength of Ships Running Among Waves," SNA of Japan, 1951.
8. DeDoes, J.C.: "Experimental Determination of Bending Moments for Three Models of Different Fullness in Regular Waves," Report 36S, Netherlands Research Center, T.N.O. for Shipbuilding and Navigation, April 1960.
9. Lutz, P.C. and Kimball, E.D.: "Ship Model Bending Moments in Waves," Thesis: Department of Naval Architecture, M.I.T., May 1957.
10. Dalzell, J.F.: "Effect of Speed and Fullness on Hull Bending Moments in Waves," DL Report 707, February 1959.
11. Dalzell, J.F.: "Some Further Experiments on the Application of Linear Superposition Techniques to the Responses of a Destroyer Model in Extreme Irregular Long-Crested Head Seas," DL Report 918, September 1962.

NOMENCLATURE

| | |
|----------------|--|
| Arg: | = Argument |
| A_2 | = Coefficient in equation of \bar{M}_{FA} |
| a,b,N | = Coefficients |
| B | = Maximum Model Beam |
| C | = Non-Dimensionalized Bending Moment (Bending Moment/ $\rho g L^2 B h$) |
| C_2 | = Coefficient in equation of \bar{M}_{FA} |
| C_B | = Block Coefficient |
| C_{θ} | = Midsection Coefficient |
| d | = Duration of Response to Half Sine Pulse, at Midheight |
| D | = Duration of Half Sine Pulse |
| E | = Maximum Response of Measuring System to Half Sine Pulse |
| g | = Acceleration due gravity |
| H | = Draft |
| h | = Wave Height |
| h/λ | = Wave Steepness |
| K_o | = Longitudinal Gyradius |
| L | = Model length on 20 stations |
| LBP | = Length between Perpendiculars |
| LCG | = Longitudinal Center of Gravity |
| M | = Bending Moment, General |
| \bar{M}_{FA} | = Average Midship Bending Moment Due to Acceleration of Model Mass |

| | |
|-------------------------|--|
| \bar{M}_{RE} | = Part of \bar{M}_{FA} in Phase with Measured Bending Moments |
| Mod: | = Modulus |
| R | = Model Resistance in Waves |
| rms | = Root-mean Square |
| t | = Time |
| V | = Model Speed |
| VCG | = Vertical center of gravity |
| Y | = General Response |
| Z_o | = Heaving Amplitude |
| $2Z_o/L$ | = Non-Dimensional Heave Double Amplitude |
| Z_{LCG} | = Heave at LCG |
| α, β, γ | = Quantity derived in the Numerical Classification of Trends |
| Z_{pp} | = Heave at Pitchpivot |
| Δ | = Model Displacement |
| θ | = Heave Phase Angle |
| ϵ | = Pitch Phase Angle |
| θ | = Pitch Angle |
| $2\theta_o$ | = Pitch double Amplitude |
| λ | = Wave Length |
| λ/L | = Wave Length to Model Length Ratio |
| μ_H | = Hogging Moment Coefficient (hogging moment/ pgL^3B) |
| μ_S | = Sagging Moment Coefficient (sagging moment/ pgL^3B) |
| μ_H^i | = Approximate Hydrodynamic Hogging Moment ($\mu_H - \bar{M}_{RE}$) |
| μ_S^i | = Approximate Hydrodynamic Sagging Moment ($\mu_S - \bar{M}_{RE}$) |
| μ_{HA} | = Absolute Hogging Moment - Non-dimensional |
| μ_{HS} | = Absolute Sagging Moment - Non-dimensional |
| ρ | = Mass Density of Water |
| ω_e | = Frequency of Wave Encounter |

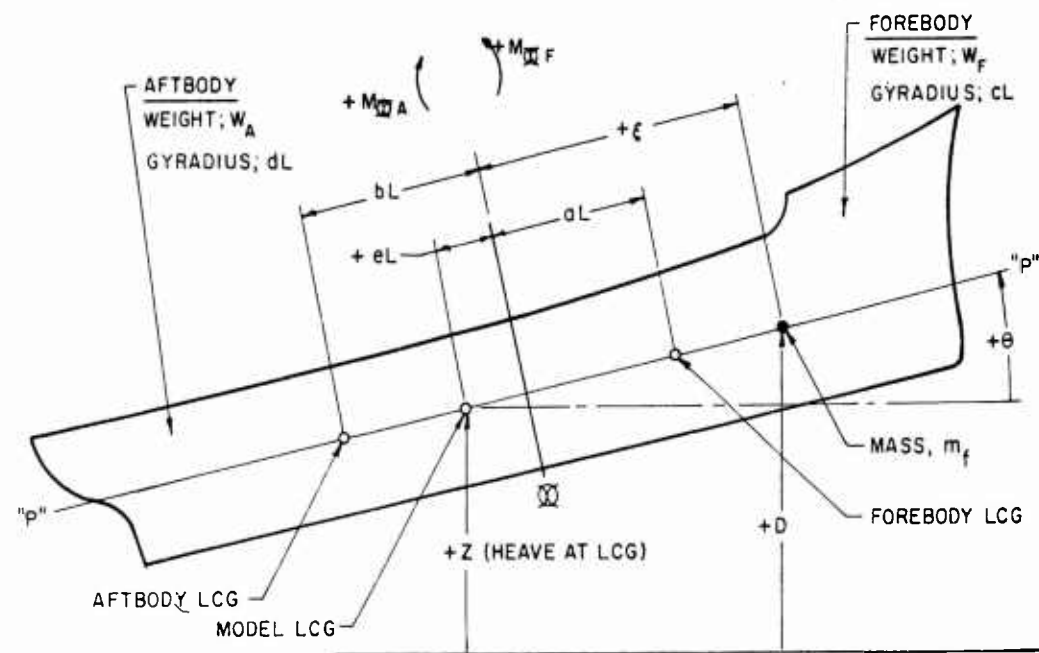


FIG. 43. NOTATION FOR DERIVATION IN APPENDIX.

APPENDIX

Approximation to the Component of Midship Bending Moment
Due to the Pitch and Heave Accelerations Imposed on the Model

A sketch showing the necessary notation is presented in Fig. 43. The model consists of two rigid bodies connected by a spring amidships. Since the actual models are relatively long and slender it is assumed that negligible error will result if all weight is assumed concentrated along a line in the center plane, parallel to the keel, and passing through the vertical center of gravity of the model. (Line $\bar{P}\bar{P}$, Fig. 43) pitching angle is assumed to be -15° or less and thus the vertical acceleration at a point on the line $\bar{P}\bar{P}$ closely approximates the normal acceleration.

Under these assumptions the midship bending moment caused by the normal acceleration of an elemental mass, m_f , (see Fig. 43) is nearly:

$$\delta M_{QF} = - \epsilon m_f \ddot{\theta} \tag{1}$$

Again under the assumption of relatively small pitch angles:

$$D = Z + (\epsilon + eL)\theta \tag{2}$$

and:

$$\ddot{\theta} = \ddot{Z} + (\epsilon + eL)\ddot{\theta} \tag{3}$$

Substituting:

$$\delta M_{QF} = - (\ddot{Z} + \ddot{\theta} eL) m_f \cdot \epsilon - \ddot{\theta} m_f \epsilon^2 \tag{4}$$

Summing the contributions from all the elements of mass in the forebody:

$$M_{\text{RF}} = - (\ddot{Z} + \ddot{\theta} eL) \sum_0^{L/2} m_F \xi - \ddot{\theta} \sum_0^{L/2} m_F \xi^2$$

$$= - (\ddot{Z} + \ddot{\theta} eL) \frac{W_F}{g} aL - \ddot{\theta} \frac{W_F}{g} (a^2 L^2 + c^2 L^2) \quad (5)$$

Similarly for the aft body with attention to the sign conventions shown in Fig. 43:

$$M_{\text{RA}} = - (\ddot{Z} + \ddot{\theta} eL) \frac{W_A}{g} bL + \ddot{\theta} \frac{W_A}{g} (b^2 L^2 + d^2 L^2) \quad (6)$$

Rearranging:

$$M_{\text{RF}} = - A_1 \left(\frac{2\ddot{Z}}{L} \right) - C_1 (2\ddot{\theta}) \quad (7)$$

$$M_{\text{RA}} = - B_1 \left(\frac{2\ddot{Z}}{L} \right) - D_1 (2\ddot{\theta}) \quad (8)$$

where:

$2\ddot{\theta}$ is in degrees/sec²

$$A_1 = + aW_F L^2/2g \quad \text{Ft Lb Sec}^2$$

$$B_1 = + bW_A L^2/2g \quad \text{"}$$

$$C_1 = (ae + a^2 + c^2)W_F \cdot L^2 \pi/360g \quad \frac{\text{Ft Lb Sec}^2}{\text{Degree}}$$

$$D_1 = (be - b^2 - d^2)W_A \cdot L^2 \pi/360g \quad \text{"}$$

Assuming harmonic motions

$$\ddot{Z} = - \omega_e^2 Z_0 \cos(\omega_e t - \delta) \quad (9)$$

$$\ddot{\theta} = - \omega_e^2 \theta_0 \cos(\omega_e t - \epsilon) \quad (10)$$

Where δ and ϵ are phase lags of maximum upward motion after maximum sagging moment and ω_e is the wave encounter frequency.

Substituting (9) and (10) into (7) and (8), expanding and re-arranging:

$$M_{\text{RF}} = \left[A_1 \omega_e^2 \left(\frac{2Z_0}{L} \right) \cos \delta + C_1 \omega_e^2 (2\theta_0) \cos \epsilon \right] \cos \omega_e t$$

$$+ \left[A_1 \omega_e^2 \left(\frac{2Z_0}{L} \right) \sin \delta + C_1 \omega_e^2 (2\theta_0) \sin \epsilon \right] \sin \omega_e t \quad (11)$$

$$M_{\text{RA}} = \left[B_1 \omega_e^2 \left(\frac{2Z_0}{L} \right) \cos \delta + D_1 \omega_e^2 (2\theta_0) \cos \epsilon \right] \cos \omega_e t$$

$$+ \left[B_1 \omega_e^2 \left(\frac{2Z_0}{L} \right) \sin \delta + D_1 \omega_e^2 (2\theta_0) \sin \epsilon \right] \sin \omega_e t \quad (12)$$

($2\theta_0$ in Degrees)

Since ships do not generally have their LCG at amidship A_1 and B_1 are not usually equal. C_1 and D_1 are usually unequal for about the same reason. Thus

$$M_{RF} \neq M_{RA} \text{ (usually)}$$

The bending moments from all sources forward of amidships must equal those from sources aft of amidships.

If: H_{RF} and H_{RA} denote hydrodynamic bending moments:

And: M_R = Total midship moment

$$\begin{aligned} M_R &= M_{RF} + H_{RF} = M_{RA} + H_{RA} \\ &= \frac{M_{RF} + M_{RA}}{2} + \frac{H_{RF} + H_{RA}}{2} \end{aligned} \quad (13)$$

In order to simplify the analysis, the average of the forward and aft moments due to acceleration of model mass was calculated:

$$\begin{aligned} \bar{M}_{FA} &= \left[A_2 \omega_e^2 \left(\frac{2Z_0}{L} \cos \delta \right) + C_2 \omega_e^2 (2\theta_0 \cos \epsilon) \right] \cos \omega_e t \\ &+ \left[A_2 \omega_e^2 \left(\frac{2Z_0}{L} \sin \delta \right) + C_2 \omega_e^2 (2\theta_0 \sin \epsilon) \right] \sin \omega_e t \end{aligned} \quad (14)$$

where:

$$A_2 = (aW_F + bW_A) L^2 / 4g$$

$$C_2 = \left[(ae + a^2 + c^2)W_F + (be - b^2 - d^2)W_A \right] \cdot L^2 \pi / 720g$$

($2\theta_0$ in Degrees)